2009

Role of KCNMA1 in the Pathogenesis of Gepd Syndrome

Wei Du
Cleveland State University

ROLE OF KCNMA1 IN THE PATHOGENESIS OF GEPD SYNDROME

WEI DU

Bachelor of Science in Biochemistry

Beijing Normal University

June, 2001

Submitted in partial fulfillment of requirements for the degree

DOCTOR OF PHILOSOPHY IN REGULATORY BIOLOGY

at the

CLEVELAND STATE UNIVERSITY

NOVEMBER, 2009

This dissertation has been approved

for the Department of Biological, Geological, and Environmental

Sciences and the College of Graduate Studies by

_____

Dissertation Chairperson, Qing Wang

_____

Department & Date

_____

Crystal Weyman

_____

Department & Date

_____

Sadashiva Karnik

_____

Department & Date

_____

Xiaoxia Li

_____

Department & Date

_____

Roman Kondratov

_____

Department & Date

_____

Qiuyun Chen

_____

Department & Date

ACKNOWLEDGEMENT

I would like to thank my advisor, Dr. Qing Wang, for his help and support. I want to thank my committee members, Dr. Crystal Weyman, Dr. Sadashiva

Karnik, Dr. Xiaoxia Li, Dr. Roman Kondratov, and Dr. Qiuyun Chen, for their time and effort. I want to thank Dr. Jocelyn Bautista for collecting the blood samples from the patients. I want to thank our collaborators, Dr. Jianmin Cui, Dr. George Richerson, Dr. Huanghe Yang, and Dr. Ana Diez-Sampedro. I want to thank Dr. Chun Fan for teaching me some molecular techniques, and I want to thank Dr. Teng Zhang for teaching me some mouse techniques. I want to thank all Wang lab members that helped me.

ROLE OF KCNMA1 IN THE PATHOGENESIS OF GEPD SYNDROME

WEI DU

ABSTRACT

The coexistence of generalized epilepsy and paroxysmal dyskinesia within the same individual is an increasingly recognized neurological syndrome, with both sporadic and familial cases reported. The basic pathophysiology underlying GEPD is unknown, and no specific genes have been identified for it. In order to identify genes associated with GEPD, a genome-wide linkage scan was carried out in a Caucasian family affected by GEPD. A disease locus was mapped on chromosome 10q22 and a mutation was identified in KCNMA1 encoding the pore-forming α–subunit of the large conductance calcium-activated potassium channel (BK channel). The mutant BK channel showed a markedly greater macroscopic current and an increase in calcium sensitivity. We propose that enhancement of BK channels in vivo leads to increased excitability by inducing rapid repolarization of action potentials, resulting in GEPD by allowing neurons to fire at a faster rate. These results identify a gene that is mutated in GEPD and support the role of ion channels in the pathogenesis of this syndrome.

TABLE OF CONTENTS

LIST OF TABLES

Table Page

LIST OF FIGURES

CHAPTER I

INTRODUCTION

1.1 Channelopathies in Epilepsy

Epilepsy is one of the most common chronic neurological disorders, affecting about 50 million people worldwide (1). It is characterized by recurrent unprovoked seizures, and increases risk of trauma and sudden death (2). Epileptic seizures are transient occurrence of signs and/or symptoms due to abnormal excessive or synchronous neuronal activity in the brain (3). Epilepsies are classified into three groups by location or distribution of seizures and by causes. Partial or focal epilepsies arise from a small portion of the brain that drives the epileptic response. Generalized epilepsies, in contrast, arise from epileptic circuits that involve the whole brain. The third group is epilepsies of unknown localization (4).

Mutations in over seventy genes have been linked to different types of epilepsies. Many of these identified genes encode ion channels, suggesting ion channel defects as a genetic cause of epilepsies (Table I).

Multiple voltage-gated sodium channel mutations have been identified in epileptic patients. Sodium channels are composed of α and β subunits. The α subunits are transmembrane proteins with four homologous domains. They contain voltage sensors and pore regions (5). The β subunits bind to the α subunits and regulate cell surface expression, voltage dependence, and kinetics of the α subunits (6).

A mutation in the sodium channel β1 subunit gene *SCN1B* was identified in an Australian family with generalized epilepsy with febrile seizures plus (GEFS+) (7). The mutation results in impaired modulation of sodium channel function (8). In 2000, GEFS+ patients in two families were found to carry mutations in *SCN1A* encoding the α1 subunit (9). Subsequently, eleven additional *SCN1A* mutations were reported in GEFS+ families (10). *SCN1A* mutations were also identified in patients affected by severe myoclonic epilepsy of infancy (SMEI) (11).

The *SCN1A* mutations alter sodium channel functions in several different ways. Three mutations (T875M, W1204R, and R1648H) lead to impaired channel inactivation and an increased persistent current. In neurons, this persistent current may reduce depolarization threshold of action potentials, resulting in neuronal hyperexcitability (12). The interaction between the α and β subunits was impaired by the D1866Y mutation. It was shown that neurons expressing mutant channels fire an action potential at a higher frequency (13). R1648H mutant channels displayed an increased rate

Table I. Ion channels implicated in epilepsy

Channel	Gene	Syndrome
Sodium channel	SCN1A	Generalized epilepsy with febrile seizures plus
	SCN2A	Benign familial neonatal infantile seizures
	SCN1B	Generalized epilepsy with febrile seizures plus
Potassium channel	KCNQ1	Episodic ataxia type 1 and partial epilepsy
	KCNQ2	Benign familial neonatal convulsions
	KCNQ3	Benign familial neonatal convulsions
	KCNAB2	Severe seizures
Calcium channel	CACNA1A	Generalized epilepsy
	CACNB4	Generalized epilepsy and episodic ataxia
Chloride channel	CLCN2	Idiopathic generalized epilepsy

of recovery from inactivation, another route to hyperexcitability (14).

Mutations in *SCN2A* are not common as *SCN1A* in epileptic patients. Only a few mutations have been identified in patients with benign familial neonatal infantile seizures (15, 16). The underlying molecular mechanisms remain to be investigated.

The KCNQ family of voltage-activated potassium channels plays an important role in repolarization of action potentials in cardiomyocytes, neurons and vascular smooth muscle cells (VSMCs) (17). *KCNQ2* encodes the α subunit of a potassium channel composed of six transmembrane domains and a pore region. A 5-bp insertion in the coding region of *KCNQ2* was identified in an Australian family with benign familial neonatal convulsion (BFNC) (18). The frameshift insertion results in a truncated protein with 300 less amino acids that was unable to produce currents when expressed in cells. Loss-of-function of the mutant KCNQ2 channel leads to impaired repolarization, which is likely to be the molecular mechanism for the pathogenesis of BFNC. In addition, six other mutations in *KCNQ2* were later reported that are associated with BFNC (19).

Two other genes of this family, *KCNQ1* and *KCNQ3*, have also been linked to epilepsies. A Gly263Val missense mutation was identified in the pore region of KCNQ3 channel in a Mexican-American family with BFNC (20). This mutation was hypothesized to alter excitability of the cells through the same pathway as *KCNQ2*. A Thr226Arg mutation was identified in the second

transmembrane domain of the KCNQ1 channel in the patients affected by both episodic ataxia type 1 and partial epilepsy (21). Electrophysiological studies showed that expression of the mutant KCNQ1 channels in cells significantly decreased the peak currents, which were only about 3% of those of the wild-type channels. Mice lacking KCNQ1 channels displayed frequent spontaneous seizures which are the characteristic of epilepsies. Electrophysiological studies indicated that action potentials are induced at a lower threshold in nerve cells lacking KCNQ1 and the axonal conduction of action potentials was also altered (22,23).

Loss of the regulatory β subunit KCNAB2 in eight patients resulted in severe seizures (24). The *KCNAB2* knockout mice displayed occasional seizures which are similar to those observed in *KCNQ1* knockout mice (25). Loss of the β subunit might prolong membrane repolarization.

CACNA1A is a voltage-gated P/Q-type calcium channel expressed in the brain. A C5733T mutation was identified in *CACNA1A,* and resulted in a truncated protein without the C-terminal region of the channel in patients with generalized epilepsy (26). Electrophysiological studies indicate that the mutation impaired channel function in a dominant negative fashion. *CACNA1A* knockout mice developed rapidly progressive neurological deficit with specific characteristics of ataxia and dystonia (27). Further studies demonstrated that calcium currents were completely eliminated in cerebellar granule cells. Synaptic transmission was not affected but showed enhanced

reliance on N-type and R-type calcium channels, indicating that CACNA1A is also involved in synaptic transmission.

Two mutations have been identified in the β4 subunit gene of the voltage-gated calcium channel *CACNB4* in families with idiopathic generalized epilepsy and episodic ataxia. C104F is a missense mutation, and R482X results in a truncated protein lacking 38 amino acids in the C-terminal domain (28). Expression of the R482X mutant protein in *Xenopus* oocytes showed slowed inactivation of the calcium channels. Considering that the truncation site is located in the domain interacting with the pore-forming α subunit, it is likely that the mutant β subunit alters channel functions by impairing its association with the α subunit.

The ducky mouse is a model of absence epilepsy characterized by spike-wave seizures and ataxia. Genetic analysis of the ducky mice identified two mutations in the *Cacna2d2* gene encoding the α2δ2 voltage-dependent calcium channel subunit. Both mutations were predicted to cause loss of the full length α2δ2 protein (29). Because normal α2δ2 subunit increases the maximum conductance of the pore-forming α subunit in combination with the β4 subunit, it is likely that loss of the α2δ2 subunit in ducky mice is responsible for the reduced calcium channel currents in cerebellar Purkinje cells of the ducky mice.

Three mutations have been identified in the chloride channel gene *CLCN2* in three unrelated families with idiopathic generalized epilepsy (IGE).

The mutations include a single-nucleotide frameshift insertion (M200fsX231), a 11-bp deletion in intron 2 resulting in a splicing variant lacking exon 3 (Delexon3), and a missense mutation (G715E) (30). Normal CLCN2 channels are activated during the hyperpolarization phase of the cell membrane by both membrane potential and intracellular chloride. Expression of the M200fsX231 and Delexon3 mutant channels did not produce detectable currents, indicating loss-of-function for both mutations. G715E mutant channels generated normal currents, but they were activated at less negative potentials at a given chloride concentration.

Many non-ion channel genes also contribute to the pathogenesis of epilepsy. Mice deficient of genes encoding synaptic vesicle-related proteins synapsins and SV2 experienced severe seizures (179, 180). Gamma-Aminobutyric acid (GABA) is an inhibitory neurotransmitter in the central nervous system. Multiple genes involved in GABA synthesis contribute to epileptic phenotypes, including *GAD65* (181), *EAAT1* (182) and *TNAP* (183). Mutations in genes encoding different GABA receptor subunits have been associated with epilepsy (184-188). Some other neurotransmitter receptors also play a role in epilepsy, including glutamate (189), acetylcholine (190), and serotonin receptors (191, 192).

1.2 Paroxysmal Dyskinesia

Paroxysmal dyskinesias (PD) are a heterogeneous group of neurological

disorders characterized by recurrent brief episodes of abnormal involuntary movements (31). PD can be classified into three main groups.

Paroxysmal kinesigenic dyskinesia (PKD) occurs in early childhood and its attack frequency often decreases as the patients grow up. PKD is induced by sudden movements or change in velocity (going from walking to running). PKD patients have frequent attacks everyday and respond dramatically to low doses of carbamazepine (32). Paroxysmal nonkinesigenic dyskinesia (PNKD) is characterized by spontaneous attacks induced by alcohol, caffeine, stress, or fatigue. PNKD is not as frequent as PKD, but it can last up to six to eight hours in some cases (33). Paroxysmal exercise-induced dyskinesia (PED) usually occurs after ten to fifteen minutes of continuing exercise, which is different from PKD that is caused by initiation of movement. PED often occurs in the legs after prolonged walking or running (34).

Like epilepsies, ion channel genes have also been linked to paroxysmal dyskinesias. Four different missense mutations were identified in *KCNA1* encoding a voltage-gated potassium channel, in patients with movement disorders (35). A brain-specific P/Q-type calcium channel α1-subunit gene *CACNL1A4* was linked to patients with hemiplegic migraine and episodic ataxia type-2, which has some clinical features similar to PD. Several missense and frameshift mutations in the functional domains, as well as polymorphism sin the 3'-UTR, were identified in *CACNL1A4* (36). Together with ion channel mutations identified in epilepsies, these results strongly

suggest that ion channel defects play an important role in pathogenesis of neurological diseases.

Non-ion channel genes have also been associated with paroxysmal dyskinesia. In 2004, mutations in the myofibrillogenesis regulator 1 gene *MR1* were identified in fifty patients affected by paroxysmal non-kinesigenic dyskinesia from eight families (193). Recently, mutations in *SLC2A1*, encoding the glucose transporter type 1, were reported to cause paroxysmal exercise-induced dyskinesia (194, 195).

Linkage analysis mapped another genetic locus for PNKD to chromosome 2q31-36, but no specific gene has been identified (37, 38). Interestingly, a cluster of sodium channel genes are located within this region. PKD was linked to chromosome 16p12-q12 in several different families (39, 40). Although the specific gene causing PKD is unknown, this chromosomal region contains ion channel genes, which may be good candidates for mutational screening.

1.3 Coexistence of Epilepsy and Paroxysmal Dyskinesia

Epilepsy and paroxysmal dyskinesia are two distinct disorders with some shared clinical features. PD patients lack both EEG abnormalities and episodes of unresponsiveness during attacks that are found in epilepsy patients (41). The coexistence of epilepsy and paroxysmal dyskinesia within the same individual is an increasingly recognized neurological syndrome, with

both sporadic and familial cases reported (42, 43).

ICCA is a syndrome characterized by infantile seizures and paroxysmal kinesigenic dyskinesia (PKD). Linkage analysis mapped the ICCA disease locus to a 10 cM pericentromeric region on chromosome 16 (44, 45). One family with rolandic epilepsy and paroxysmal exercise-induced dyskinesia (PED) was also linked to chromosome 16. The 6 cM disease locus is entirely included in the ICCA locus, suggesting the same gene could be responsible for both syndromes (46). Some other reports also linked coexistent epilepsy and PKD to chromosome 16 in different populations (47, 48).

These results strongly suggest the pericentromeric region of chromosome 16 is tightly linked to epilepsy/PKD as well as epilepsy/PED, but no specific gene in this region has been identified. Moreover, no genetic locus has been mapped for coexistent epilepsy and paroxysmal nonkinesigenic dyskinesia (PNKD). Ion channel defects may play an important role in the pathogenesis of coexistent epilepsy and PD, as demonstrated in different types of epilepsy and paroxysmal dyskinesia.

1.4 BK Channel

BK channels are activated by both membrane voltage and intracellular calcium (49). They are expressed in many cell types including neurons (50), hair cells (51), skeletal and smooth muscle cells (52, 53). BK channels play important roles in a variety of physiological processes, such as neural

transmission, muscle contraction and hearing. The pore-forming α subunit of BK channel contains seven transmembrane domains (S0-S6) at the N-terminus, a voltage-sensor (S1-S4), and a pore gate between S5 and S6. The cytosolic C-terminal domain of BK channels has four hydrophobic segments (S7-S10), the calcium bowl and the RCK (regulator of conductance for K^+) domain (54) (Figure 1). The calcium bowl is a high-affinity calcium binding site (55), and the RCK domain contains binding sites for calcium and magnesium (56, 57).

Four residues in the voltage-sensing domains (S1-S4) of the mouse BK channel have been identified as the voltage-sensing residues: Asp153 and Arg167 in S2, Asp186 in S3 and Arg213 in S4 (58). BK channels are less sensitive to membrane voltage compared to voltage-gated potassium channels such as Shaker, which has 12-13 effective gating charges (59). BK channels can be activated by membrane voltage in the absence of calcium (60). Like voltage-gated potassium and sodium channels, membrane voltage causes the displacement of the charged residues in the voltage-sensing domains, inducing channel opening (61).

BK channels can also be activated by binding of intracellular calcium to its cytosolic domain, and the activation can be independent of membrane voltage (62). There are at least two calcium binding sites in the cytosolic domain of the pore-forming α subunits of the BK channel. One site is known as the calcium bowl which contains a series of Asp residues, and the other

site is located within the RCK domain (56). A model was proposed to explain the coupling between calcium binding and channel opening. Binding of calcium to the multiple binding sites changes the conformation of the RCK domain. As a result of the conformational change, the gating ring expands to increase in diameter resulting in channel opening (63).

Although both voltage and calcium can activate BK channels independently, there are interactions between the two factors mediated by channel opening. It was shown that opening of the channel gate by one factor enhances the effect of the other (64).

Malfunction of BK channel leads to many diseases. Mice lacking the α subunit of BK channel has abnormal conditioned eye-blink reflex and abnormal locomotion and motor coordination (65). These mice also developed high-frequency hearing loss at eight weeks of age (66). The β4 subunit of BK channel broadens action potentials by preventing the α subunit from inducing the repolarization phase of the action potential. β4 knockout mice displayed distinctive seizures emanating from the temporal cortex, and the granule cells from these mice had a higher firing frequency (67). The calcium sensitivity of BK channel was reduced in mice deficient for the β1 subunit, and the mice showed an increase in arterial tone and blood pressure (68). A single nucleotide polymorphism C818T in the β1 subunit was found to be associated with asthma in African American male asthmatics (69).

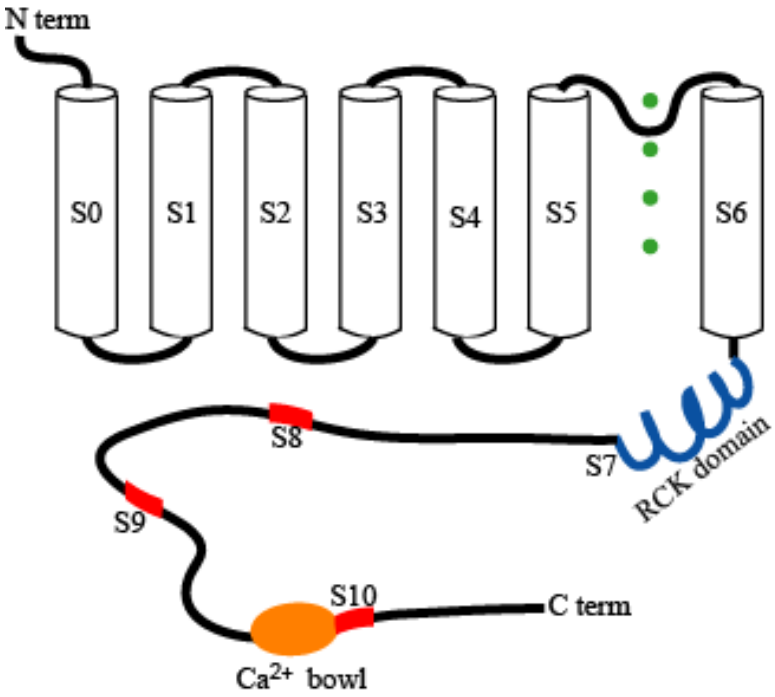

Figure 1. Structure of the BK channel. The BK channel contains seven transmembrane domains (S0-S6), a pore gate between S5 and S6, four hydrophobic segments (S7-S10), the calcium bowl and the RCK domain.

In summary, these results suggest that BK channel α subunit, as well as its auxiliary β subunits, play important roles in a variety of physiological processes.

CHAPTER II

D434G MUTATION OF KCNMA1 IN GEPD FAMILY

2.1 Abstract

The coexistence of epilepsy and paroxysmal dyskinesia in the same individual or family is an increasingly recognized phenomenon. The purpose of this study was to identify the gene that is mutated in generalized epilepsy and paroxysmal dyskinesia (GEPD) in an American family. Genomic DNA was solated from blood of the family members. A genome-wide linkage scan with 382 microsatellite markers identified a disease locus on chromosome 10q22. Fine mapping and haplotype analysis using eight additional markers defined the disease-associated interval to a region of 8.4 cM flanked by markers *D10S1694* and *D10S201*. Candidate genes in this region was screened for mutations by sequencing and a heterozygous point mutation A1301G was identified in exon 10 of *KCNMA1*, encoding the pore-forming α subunit of BK channel. The A1301G mutation results in the substitution of a negatively

solated from blood of the family members. A genome-wide linkage scan with 382 microsatellite markers identified a disease locus on chromosome 10q22. Fine mapping and haplotype analysis using eight additional markers defined the disease-associated interval to a region of 8.4 cM flanked by markers *D10S1694* and *D10S201*. Candidate genes in this region was screened for mutations by sequencing and a heterozygous point mutation A1301G was identified in exon 10 of *KCNMA1*, encoding the pore-forming α subunit of BK channel. The A1301G mutation results in the substitution of a negatively charged aspartic acid residue for a neutral glycine residue (D434G) in the regulator of conductance for K^+ (RCK) domain. A1301G was present in 13 affected individuals and absent in 5 unaffected individuals in the family. Furthermore, the mutation was not detected in 500 unrelated healthy controls. Together, these results suggest that A1301G in *KCNMA1* is responsible for GEPD in this family.

2.2 Introduction

Epilepsy is one of the most common chronic neurological disorders, affecting about 50 million people worldwide (1). It is characterized by recurrent unprovoked seizures, and increases risks of trauma and sudden death (2). Mutations in over seventy genes have been linked to different types of epilepsies. Many of these identified genes encode ion channels, suggesting ion channel defects as a genetic cause of epilepsies (Table I).

Paroxysmal dyskinesias (PD) are a heterogeneous group of neurological disorders characterized by recurrent brief episodes of abnormal involuntary movements (31). Epilepsy and paroxysmal dyskinesia are two distinct disorders with some shared clinical features. PD patients lack both electroencephalography (EEG) abnormalities and episodes of unresponsiveness during attacks that are found in epilepsy patients (41). Like epilepsy, ion channel genes have also been linked to paroxysmal dyskinesias (35, 36).

The coexistence of epilepsy and paroxysmal dyskinesia within the same individual is an increasingly recognized neurological syndrome, with both sporadic and familial cases reported (42, 43). Previous results suggest the pericentromeric region on chromosome 16 is tightly linked to coexistent epilepsy and paroxysmal dyskinesia (45-48), but no specific gene in this region has been identified.

Here we report that a region of 8.4 cM flanked by markers *D10S1694* and *D10S201* on chromosome 10q22 is associated with coexistent generalized epilepsy and paroxysmal dyskinesia in an American family, and show that a point mutation in the BK channel α subunit gene *KCNMA1* co-segregates with affected individuals in the family. These findings identify a new genetic locus and a candidate gene for GEPD.

2.3 Materials and Methods

This study was approved by the Cleveland Clinic Institutional Review Board on Human Subjects. Informed consent was obtained from all participants or their guardians. The patients and family members were identified and clinically characterized at the Department of Neurology of the Cleveland Clinic Foundation. The family under study is of mixed European descent, and was referred to this study from the adult epilepsy clinic due to the diagnosis of epilepsy in multiple family members. A detailed pedigree was constructed. Clinical information was obtained through semistructured interviews in person and over the phone, conducted by a neurologist with specialty training in epilepsy and clinical neurophysiology. Seizure histories were corroborated by questioning eyewitnesses where possible. Records of interictal EEG and video-EEG were obtained when applicable. Epilepsy was defined as two or more unprovoked seizures. Seizure types were classified according to the International Classification of Epileptic Seizures. Epilepsy syndromes were classified according to the International Classification of Epilepsies and Epileptic Syndromes.

The proband (IV-8) was interviewed at 21 years of age. She had normal birth and early development. Routine neurological exam was normal. At two years of age she developed episodes of involuntary mouth movement and hand stiffness, lasting 10 seconds to two minutes, with preserved consciousness; these occurred weekly, were more common with fatigue,

were not triggered by sudden movement, and were diagnosed as PD. At approximately the same age she developed separate episodes of loss of awareness, with vacant staring and unresponsiveness, characteristic of typical absence seizures. There was no aura, and these absence seizures occurred daily in early childhood, progressively decreasing in frequency to monthly seizures in adolescence, on medication. Routine EEG showed generalized spike-wave-complexes.

Her paternal first cousin (IV-1) had episodes of vacant staring and episodes of PD without loss of awareness. She was evaluated with inpatient continuous video-EEG. Her interictal EEG showed generalized spike-wave complexes. Episodes of vacant staring and eyelid fluttering were associated with bursts of generalized spike-wave complexes, confirming their epileptic nature. Episodes of PD were not associated with any EEG change, confirming their non-epileptic nature. At five years of age she developed generalized tonic-clonic seizures.

Epileptic seizures, in those other family members affected with epilepsy, were typically absence seizures, with generalized tonic-clonic seizures in two other individuals (IV-1, IV-2). The age of onset of absence seizures in the family is earlier than usual for typical absence seizures, but such an early age of onset has been described in a series of patients with coexistent absence epilepsy and paroxysmal dyskinesia. The seizure types exhibited by this family did not have any resemblance to benign familial neonatal seizures or

benign infantile convulsions. There was no clear evidence for myoclonic seizures in any of the affected individuals.

The proband's seizures were responsive to valproate and lamotrigine. The seizure frequency in the proband has varied from daily (when she was younger and not taking medications regularly) to monthly (her seizure frequency in current years on valproate and/or lamotrigine). Individuals IV-1 and IV-2 had seizures and PD partially responsive to clonazepam.

PD can be broadly classified into two main subtypes: paroxysmal kinesigenic dyskinesia (PKD) if the attacks are induced by sudden movement and paroxysmal non-kinesigenic dyskinesia (PNKD) if they are not. PD, in those affected, were often described as involuntary dystonic or choreiform movements of the mouth, tongue, and extremities, non-kinesigenic but induced by alcohol, fatigue, and stress, most consistent with PNKD. PNKD in this family had onset in childhood and showed a gradual decrease in frequency with age, but persisted into the fourth decade in some individuals. The human subjects had no complaints of hearing loss or other neurological symptoms and had no evidence for hearing loss on routine neurological exams.

Human genomic DNA was prepared from whole blood with the DNA Isolation Kit for Mammalian Blood (Roche Diagnostic Co). Genome-wide genotyping was carried out using 382 polymorphic, fluorescently labeled microsatellite markers on chromosomes 1-22 (ABI PRISM Linkage Mapping

Set-MD10). Additional markers were identified at the Genethon database, and used for fine mapping and haplotype analysis. Markers were genotyped using an ABI 3100 Genetic Analyzer (Applied Biosystems, Foster City, CA). Allele-calling was carried out by GeneScan and GeneMapper 2 software programs (Applied Biosystems). Linkage analysis and two-point LOD score calculation were performed using the Linkage Package 5.2 assuming autosomal dominant inheritance, penetrance of 99%, a phenocopy rate of 0%, gene frequency of 1/10,000, and allele frequency of 1/n where n equals the number of alleles observed.

Mutational analysis was carried out using direct DNA sequence analysis. The genomic structure of the *KCNMA1* gene was determined by comparing the 3,537 bp cDNA sequence (GenBank accession number NM_002247) to its genomic sequence, and was found to contain 27 exons. Polymerase chain reaction (PCR) primers were then designed based on intronic sequences to amplify all 27 coding exons (Table II). PCR products were purified from agrose gels using the QIAquick PCR Purification Kit (QIAGEN, Valencia, CA) and sequenced with both forward and reverse primers by an ABI3100 Genetic Analyzer (Applied Biosystems).

Restriction fragment length polymorphism (RFLP) analysis was used to confirm the D434G mutation and to test the presence/absence of the mutation in other family members and 400 normal controls. The D434G mutation creates a *Tsp45I* restriction site. The 201bp PCR fragment containing exon 10

Table II. PCR primers for amplification of KCNMA1 exons

Exon(s)	Forward Primer (5’ to 3’)	Reverse Primer (5’ to 3’)	AT
1	AGTAGCAGCAATATGGCTGTTG	AGAAGCGGTGGGGCTGGCGCAG	60°C
2	GGTTCTTTATGGGTAGAGCATG	CTCATAAGCAAAGCCACCTTGG	58°C
3	AAACATCCTGAGGTCCAACTC	ATCAATGTAAAGGCTCATGATTG	58°C
4	GATGATACTACCTGTCATTTACC	GACTGCGAGAGCAGAGGCTG	58°C
5	TGCCAGCACCATGCTTCTCATG	ATTCTGTCCTTCAGCCATGACTC	58°C
6	AAATCAAATGGCAGACTGTGAAC	CAAGCACACCTGATATTTGCAAC	58°C
7	TGCTGTTACCCTGTAAGGCAG	AGAGGGTCTTGTTGCAGGCAAG	58°C
8	GCATGTATACACTTCAATAGCATG	GCTTCTAGTGCAGAATACAGTC	58°C
9	TATACCTTTGCAGGCCTAATCC	GAGAGGATTCTACCGCAGCAG	58°C
10	TGCAGGGTCCTGTCCGTGGT	ACCTCCACTCTTACAGACATTC	58°C
11	CTGTGGAAATTAGAGAGGAAGG	TGGCCAACCTAGGAGGTGTG	58°C
12	GAGACTACACTCGAGCATGGC	GATAGTCCTCTGCAGAAGATCC	58°C
13	CTGCCTCCTACCTCAGTCCC	AGGAAGAAGAGGCTGGACCTG	58°C
14	CCCAGAAGAAATGTTAAACAATTG	TAAGCTGTGCTCTCTACTCAAC	53°C
15	AAGAGTGTAACTCAGGTTTCCC	TCCAACTGTACCCAGCAGAGG	58°C
16	CTCTGGTCATTCAGAAGAACTG	TCAGAACGCACTCTCACCATC	58°C
17	ACAACAGTATGGTGTAGCCTTC	CCGTGGGTCAAGGTGTCTAC	58°C
18	CGTGGAGGAAATGTGGTACTC	CATACTCAAGAAAACTCTCGATG	53°C
19	GCCTTGAGTGTGTGTCCTTTG	CTTTAAGAAGCCATCTAACGATC	58°C
20	CACATCCTCTGAGATGTAATTC	CAGTATTATCCCACTGTCCAAC	58°C
21	TAGCACATAGTAAGCTCTCAG	AAGCTACAACTATTATATCCAT	58°

	C	CC	C
22	TCCCTCTCCTCTCACTTTTGC	TACTGAGTGAAGGATATCCCTC	58°C
23	GTTGTATGTATATAGTGTACTCTG	AAACCAACCTCCTCATATCCTG	58°C
24	CCTGGTCTCCCTCTGGCTTC	TGCTCTATTGGCACATCCTCC	58°C
25	TTGGATGTCGGCTGTCATGAC	ATCTGATACCACGTTCTTCAGG	59°C
26	CCCTGCTGTCCCTTGATTTTC	CCTTTACAGTAGGGGACAGG	59°C
27	GCTTTTGGTTCAGAGAGAGTTG	GTTGGAAACACCAACTGGGG	58°C

restriction enzyme *T*sp45I. The digested product was separated by 2%

agarose gels and analyzed.

2.4 Results

We studied a large family of five generations and thirty-one members with coexistent generalized epilepsy and paroxysmal dyskinesia (GEPD). The pedigree is shown in Figure 2. As paroxysmal dyskinesia in those affected family members were involuntary movements of the mouth, tongue and hands induced by alcohol, fatigue and stress, but not sudden movement, it is classified as paroxysmal nonkinesigenic dyskinesia (PNKD). Sixteen affected individuals developed epileptic seizures (n=4), PNKD (n=7) or both (n=5) (Figure 2).

The detailed clinical features of 13 affected individuals, who participated in subsequent genetic studies, are summarized in Table III. An example of interictal EEG showing generalized spike-wave complex is shown in Figure 3.

Pedigree analysis suggested that the disease is inherited in an autosomal dominant pattern in the family, because it is present in every generation and in both males and females. In order to map generic locus linked to the disease, we carried out a genome-wide linkage analysis with 382 fluorescently labeled microsatellite markers. The markers cover human chromosome 1-22 at an average interval of 10 centimorgan (cM). One centimorgan is equal to 1% chance that a marker at one locus on a

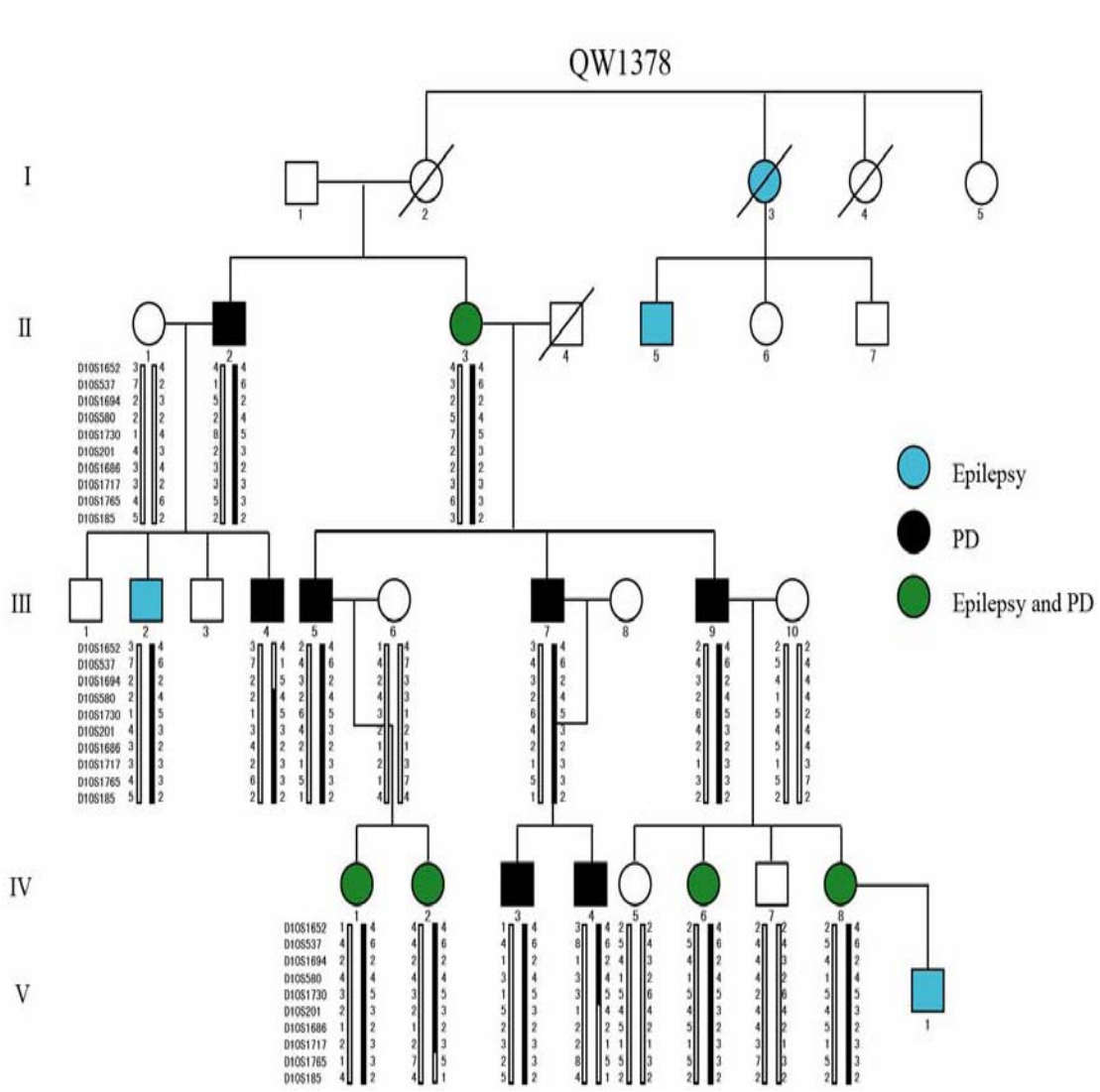

Figure 2. Genetic linkage of GEPD to chromosome 10q22 in family QW1378. Pedigree structure and genotypic analysis of the family affected with epilepsy (blue symbols), paroxysmal dyskinesia (PD; black symbols) or both (green symbols). Squares represent males; circles, females. Filled symbols denote affected individuals; open symbols, unaffected individuals. Symbols with slashes through them denote deceased individuals. The haplotype that cosegregated with the disease is indicated by a black vertical bar.

Table III. Clinical features of 13 affected individuals in family QW1378

ID	Age at onset of E	Seizure Type	EEG	Age at onset of PD	Diagnosis
II-02	--	--	--	13-15 years	PD
II-03	6 years	possible absence	normal, as adult	6 years	PD, possible E
III-02	8-9 years	possible absence	--	N/A	E
III-04	--	--	--	4-5 years	PD
III-05	--	--	normal, as adult	7 years	PD
III-07	--	--	--	4-5 years	PD
III-09	--	--	--	3-4 years	PD
IV-01	<6 months	absence, rare GTC	SWC gen	<6 months	E + PD
IV-02	3 years	absence, rare GTC	SWC gen	<6 months	E + PD
IV-03	--	--	normal	4-5 years	PD
IV-04	--	--	normal	4-5 years	PD
IV-06	5-6 years	possible absence	normal	5-6 years	PD, possible E
IV-08	2 years	absence	SWC gen	2 years	E + PD

Affected family members were diagnosed with either paroxysmal dyskinesia (PD), epilepsy (E), or both. SWC gen, generalized spike wave complexes typical of idiopathic generalized epilepsy; GTC, generalized tonic-clonic seizures.

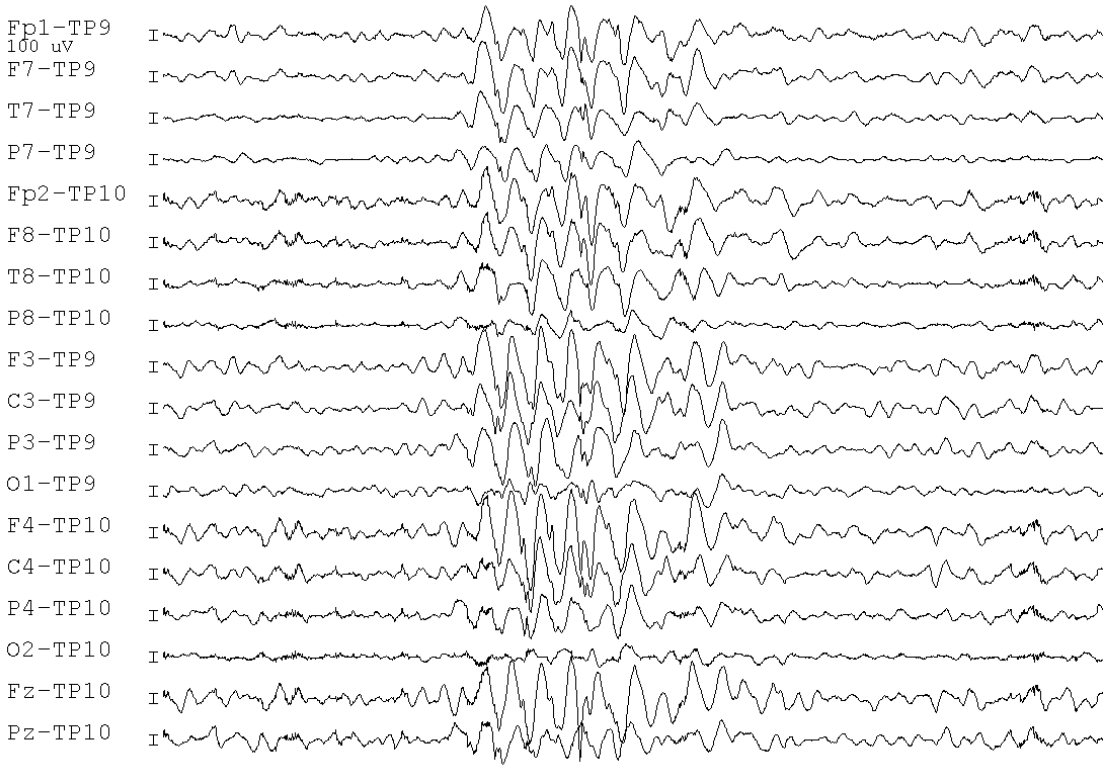

Figure 3. Representative interictal EEG of an affected member of family QW1378. EEG was recorded for individual IV-1 at 5 years of age. Ten-second EEG tracing showing interictal generalized spike-wave complexes (3-3.5 Hz) in individual IV-1 with both generalized epilepsy and paroxysmal dyskinesia.

chromosome will be separated from a marker at another locus on the same chromosome during meiosis. In genetics, cM is often used to imply distance along a chromosome, and one cM is about one million base pairs in humans.

Markers *D10S580* and *D10S1730* on chromosome 10q22 showed significant linkage to GEPD. Allele 4 of *D10S580* and allele 5 of *D10S1730* are present in all affected individuals but absent in all normal individuals in the family. The Lod score is 3.68 for marker *D10S580* and 3.73 for marker *D10S580*. Lod score calculation is a statistical test often used to determine linkage between two markers or a marker and a trait. By convention, a Lod score greater than 3.0 is considered as evidence for linkage. A Lod score of 3.0 means the likelihood that the two markers (or a marker and a trait) are not linked is less than 0.1%. Therefore, markers *D10S580* (Lod score=3.68) and *D10S1730* (Lod score=3.73) are strongly linked to GEPD. No other markers in the genome showed a Lod score of greater than 2.0, suggesting the chromosomal 10q22 region was the only region linked to GEPD.

In order to define the centromeric and telomeric boundaries for the disease-associated interval on chromosome 10q22, we carried out fining mapping and haplotype analysis using eight additional markers near *D10S580* and *D10S1730.* Individual III-4 showed a recombination between markers *D10S1694* and *D10S580*, defining *D10S1694* as the centromeric boundary for the disease-associated interval (Figure 2). Individual IV-4 had a recombination between *D10S201* and *D10S1730,* which placed *D10S201* as

the telomeric boundary for the disease interval (Figure 2). Therefore, the GEPD-associated interval in the family was mapped to a region of 8.4 cM flanked by markers *D10S1694* and *D10S201* on chromosome 10q22 (Figure 4).

We searched the Celera database for genes located in the GEPD-associated locus on chromosome 10q22. We found forty genes, including thirty-three known genes and seven hypothetical genes. Owing to the importance of ion channels in epilepsy and paroxysmal dyskinesia (discussed in Chapter I), we hypothesized that mutations in genes encoding ion channels might cause GEPD. Out of the thirty-three known genes, two of them encode ion channels. *VDAC2* encodes voltage-dependent anion channel 2, and *KCNMA1* encodes the pore-forming α subunit of the BK channel.

We carried out mutational screening of all the axons of VDAC2 and KCNMA1 by direct DNA sequence analysis. We did not find any mutation in the exons of *VDAC2*. We identified a heterozygous A to G transition in exon 10 of *KCNMA1* in an individual (IV-8) of the family (Figure 5a). The A to G transition results in the substitution of a negatively charged aspartic acid residue for a neutral glycine residue (D434G) in the regulator of conductance for K^+ (RCK) domain (Figure 5b). It has been reported that the RCK domain contains binding sites for calcium and magnesium (56, 57), thus it is likely that

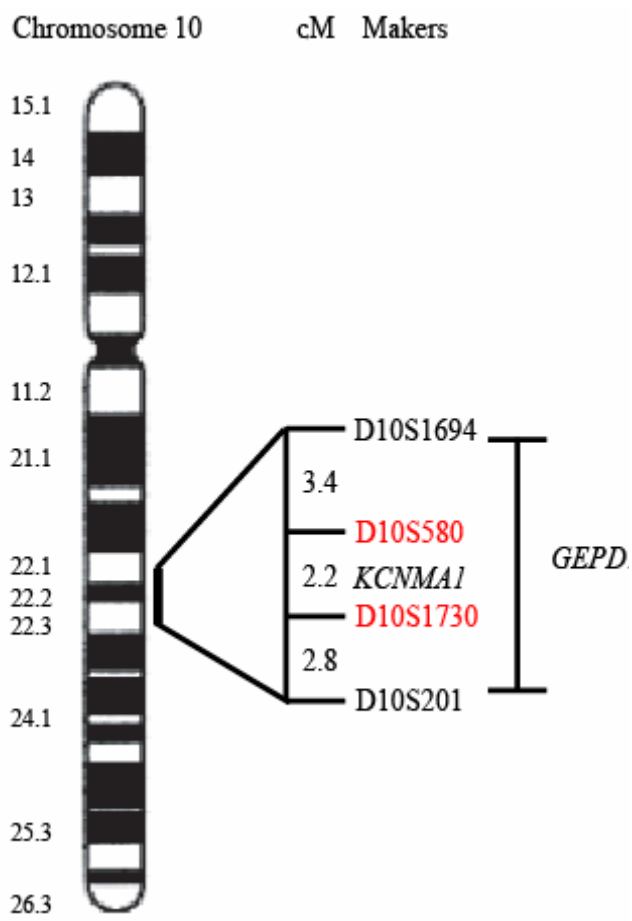

Figure 4. Location of GEPD-associated locus on chromosome 10q22. Ideogram of chromosome 10 showing Geimsa binding patterns. The GEPD-associated locus is 8.4cM flanked by markers *D10S1694* and *D10S201*. The gene *KCNMA1* is located between markers *D10S580* and *D10S1730*.

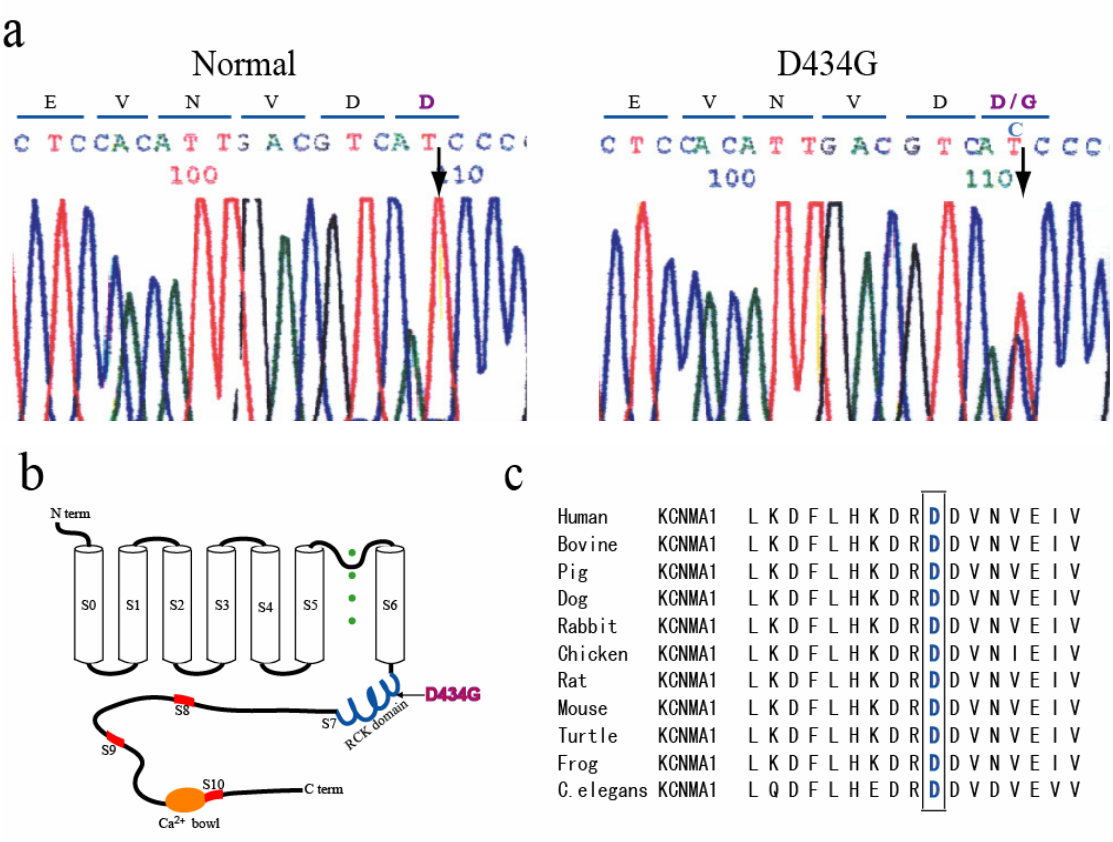

Figure 5. KCNMA1 mutation A1301G is present in individual IV-8 of family QW1378. a) DNA sequence analysis of exon 10 of *KCNMA1* from an unaffected individual (III-10) and an affected individual (IV-8) identified an A to G transition (reverse sequence) at codon 434 of individual IV-8, which results in the replacement of a negatively charged aspartic acid residue with a neutral glycine residue (D434G). b) Structure of the BK channel α subunit with D434G mutation indicated. c) Asp434 of KCNMA1 is evolutionally conserved among different species.

the D434G mutation might alter the affinity of the RCK domain to calcium or magnesium. Asp434 is located in a cluster of amino acids that are evolutionally conserved among different species (Figure 5c), suggesting the importance of this amino acid residue.

Next, we did mutational analysis of other family members whose blood samples were available. The A1301G mutation was present in all thirteen affected individuals that were genotyped and absent in five unaffected individuals in the family. The result was confirmed by restriction fragment length polymorphism (RFLP) analysis as the mutation creates a *Tsp45I* restriction site (Figure 6). Furthermore, the mutation was not detected in five hundred unrelated healthy controls. Taken together, these results suggest that the A1301G mutation of *KCNMA1* is responsible for GEPD in this large family.

We studied another family (Figure 7) by mutational analysis. We screened *KCNMA1* mutations in two family members (IV-2 and IV-3), but no mutations were found. We also carried out mutational analysis of *KCNMA1* in 102 sporadic patients with epilepsy and/or paroxysmal and no *KCNMA1* mutations were identified. There results suggest that BK channelopathy might not be a common cause for epilepsy and/or paroxysmal dyskinesia.

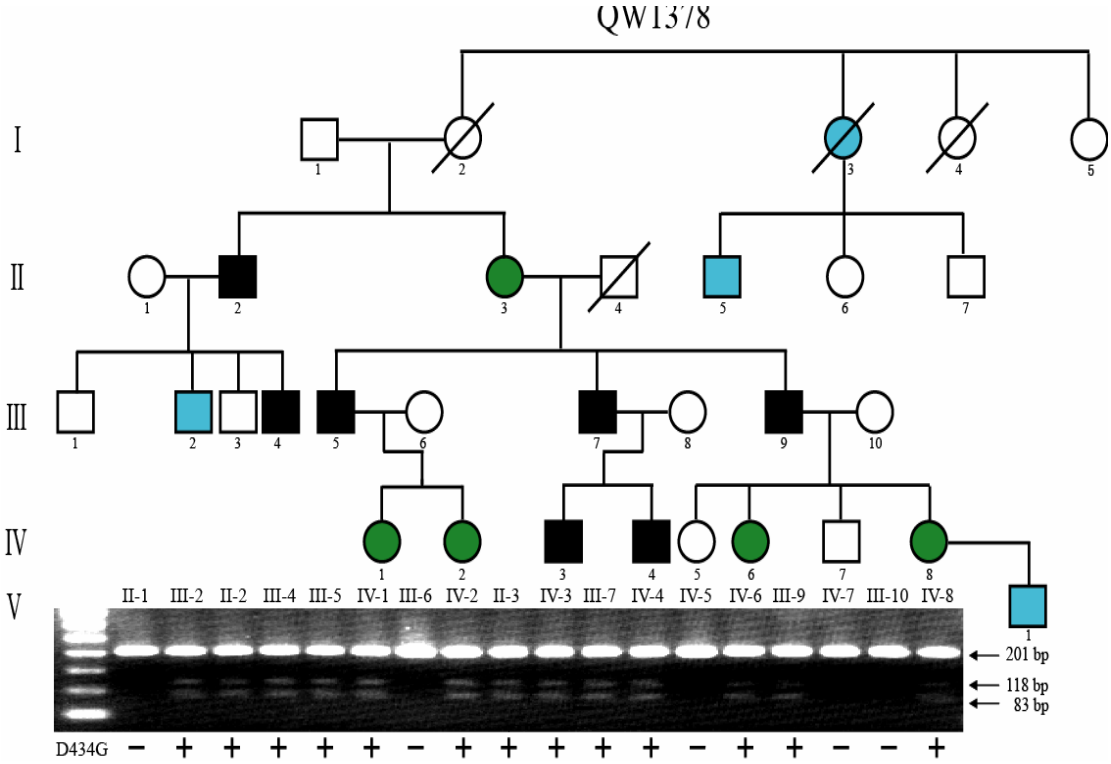

Figure 6. KCNMA1 mutation A1301G cosegregates with GEPD patients in family QW1378. The A1301G mutation creates a *Tsp45I* restriction site. The 201 bp PCR fragment containing the mutation site was digested with *Tsp45I* and separated on agarose gel. Pedigree showing clinical status is shown on the top. The results of RFLP analysis are shown below each individual. Wild type allele, 201 bp, mutant allele, 83 bp and 118 bp.

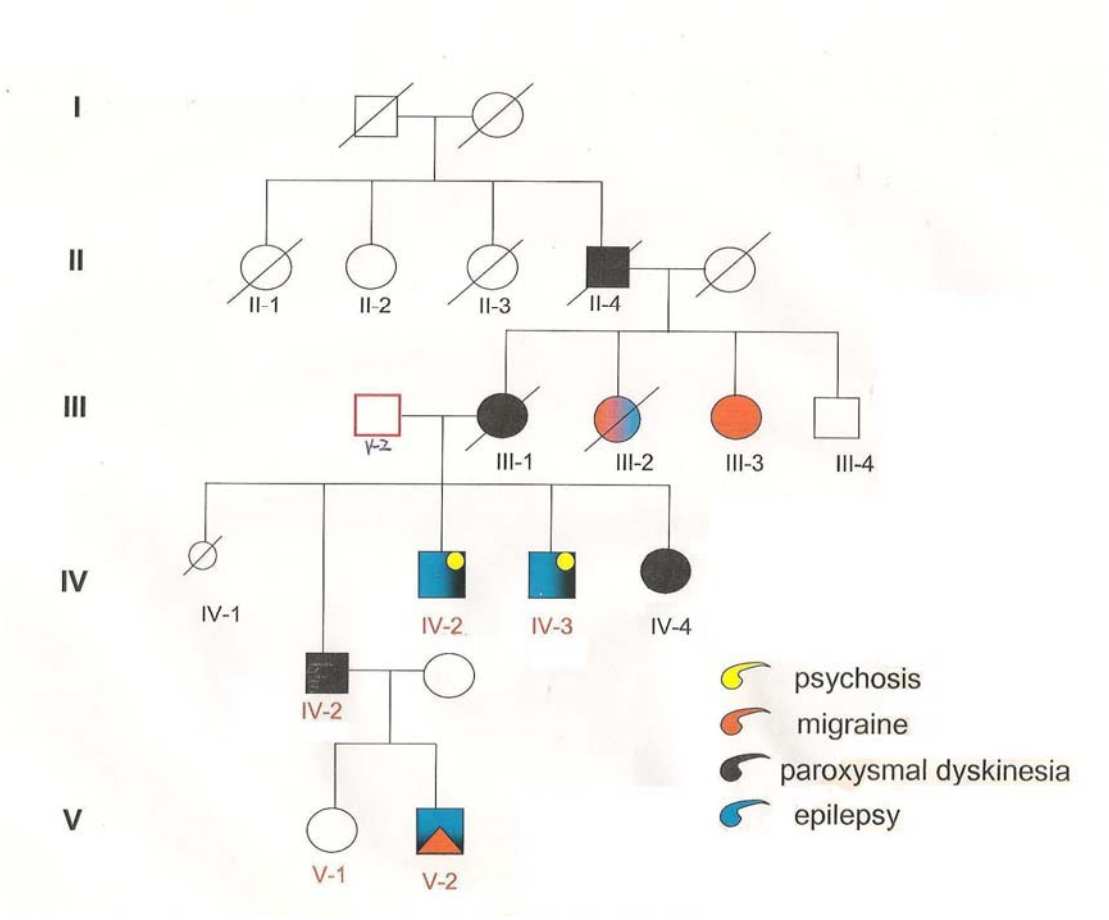

Figure 7. Pedigree of another family with coexistent epilepsy and paroxysmal dyskinesia. Different phenotypes are indicated by different colors, psychosis (yellow), migraine (orange), epilepsy (blue) and paroxysmal dyskinesia (black). Three family members (IV-2, IV-3 and V-2) have coexistent epilepsy and paroxysmal dyskinesia.

2.5 Discussion

Previous studies on coexistent epilepsy and paroxysmal dyskinesia suggest that the pericentromeric region on chromosome 16 is tightly linked to this syndrome. The genetic locus for ICCA syndrome characterized by infantile seizures and paroxysmal kinesigenic dyskinesia (PKD) was mapped to a 10 cM region on chromosome 16 (44, 45). Other reports also confirmed the linkage between the pericentromeric region on chromosome 16 and coexistent epilepsy and PKD (46-48). However, no specific gene that is mutated in the patients has been identified in this region. Thus, the KCNMA1 gene identified here is the first gene reported for coexistent epilepsy and PD.

The patients in family QW1378 were diagnosed as coexistent epilepsy and paroxysmal nonkinesigenic dyskinesia (PNKD). The linkage between the pericentromeric region on chromosome 16 to the GEPD patients in family QW1378 was excluded by our genotyping and linkage analysis. None of the microsatellite markers on chromosome 16 showed a Lod score of greater than 2.0. These results suggest that although PKD and PNKD have similar clinical features, the molecular mechanism underlying the pathogenesis of the two syndromes might be different. The 10q22 region is the first genetic locus identified for coexistent epilepsy and PNKD. Different mutations in *KCNA1* are associated with different neurological phenotypes, including partial seizures (70), but *KCNA1* mutations have not been reported as a cause of coexistent seizures and paroxysmal dyskinesia in a single individual.

Mutations in potassium channel genes *KCNQ2* and *KCNQ3* are associated with benign familial neonatal seizures (71), which are different from the absence seizures and generalized tonic-clonic seizures observed in family QW1378.

The BK channel is different from other voltage-activated potassium channels in that it can be activated by both membrane voltage and intracellular calcium. The BK channel is formed by four transmembrane α subunits. The β subunits bind to the α subunits and regulate their activities. The BK channel is a good candidate for mutational screening in GEPD patients because it plays important roles in neural transmission and muscle contraction.

The RCK domain is an intracellular motif that contains binding sites for both calcium and magnesium. The D434G mutation is located in the RCK domain, suggesting that it might be important for calcium binding. The human D434 residue corresponds to D369 of mouse KCNMA1. D369 is the second aspartic acid residue of the interloop connecting motifs αA and βB of the RCK domain. Amino acids DRDD were mutated to KSGE in mouse KCNMA1 and subjected to electrophysiological studies, and the results indicated that the four amino acids play an important role in calcium dependent activation of BK channel (67). Mutation of DRDD to KSGE has no effect on magnesium sensitivity. Therefore, D434G mutation might cause GEPD by altering calcium sensitivity of the RCK domain.

In conclusion, results from the current study demonstrate that chromosome 10q22 is tightly linked to GEPD in family QW1378 and that the A1301G mutation of *KCNMA1* cosegregates with the affected individuals in the family. Further functional characterization of the mutant BK channel may shed light on the molecular mechanism underlying the pathogenesis of GEPD.

CHAPTER III

D434G INCREASES CALCIUM SENSITIVITY OF BK CHANNEL

3.1 Abstract

Cosegregation of the D434G mutation of KCNMA1 with GEPD in family QW1378 suggests that a BK channel defect is the cause for this syndrome. The purpose of this study was to investigate the effect of the D434G mutation on BK channel function. Electrophysiological studies were performed in both *Xenopus laevis* oocytes and Chinese hamster ovary (CHO) cells using wild-type and mutant BK channels. The mutant channel had a markedly greater macroscopic current in *Xenopus laevis* oocytes. At a calcium concentration of 0.1μM and 2μM, the mutant channel was activated at lower membrane voltage. Single-channel recordings in CHO cells showed that at a given membrane voltage and calcium concentration, the mutant channel spent more time in the open state. Consistent with the results from *Xenopus laevis* oocytes, mutant BK channel was activated at lower voltage at a given calcium concentration. Together, these results suggest that the primary effect of the

D434G mutation was to increase calcium sensitivity, rather than to affect the voltage sensor, which is consistent with the role of the RCK domain as a high affinity site for calcium. It is likely that increased calcium sensitivity of the mutant BK channel leads to enhanced excitability by inducing rapid repolarization of the action potential, resulting in GEPD by allowing neurons to fire at a faster rate.

3.2 Introduction

BK channels play important roles in a variety of physiological processes, including neural transmission, muscle contraction and hearing. Mice lacking the α subunit of BK channel developed abnormal conditioned eye-blink reflex, impaired locomotion and motor coordination, and high-frequency hearing loss (65, 66). Mice deficient of the β4 subunit showed distinctive seizures (67), while the β1 subunit deficient mice showed increased arterial tone and blood pressure (68). A polymorphism in the β1 subunit was associated with asthma in African American male asthmatics (69). Despite the important physiological roles of BK channels, no mutation in the pore-forming α subunit has been associated with human disorders such as epilepsy.

The BK channel is activated by both membrane voltage and intracellular calcium. Beside the calcium bowl, the RCK domain contains high affinity sites for calcium binding, which has been demonstrated for the mouse homolog of human KCNMA1. The D434G mutation identified in family QW1378 is located

in the RCK domain of KCNMA1, suggesting it might affect the calcium sensitivity of the channel, resulting in GEPD.

Here we report the results of electrophysiological studies in both *Xenopus laevis* oocytes and mammalian CHO cells using wild-type and mutant BK channels. Greater macroscopic currents were detected in *Xenopus laevis* oocytes expressing the mutant channel. At a given calcium concentration, the mutant channel was activated at lower membrane voltage. In CHO cells, the mutant channel spent more time in the open state compared with the wild-type channel. At a given membrane voltage, the mutant channel was activated at lower calcium concentrations. Together, these results suggest that the D434G mutant BK channel has increased sensitivity to calcium.

This study establishes that the D434G mutation of the BK channel causes GEPD in family QW1378 by increasing sensitivity to calcium (a gain-of-function mechanism). It also suggests that BK channel inhibitor might be used as a potential therapy for coexistent epilepsy and paroxysmal dyskinesia.

3.3 Materials and Methods

The human *KCNMA1* cDNA was cloned into plasmid pcDNA3, resulting in an expression construct for the BK channel (kind gifts from Drs. Irwin B. Levitan and Yi Zhou at University of Pennsylvania School of Medicine and from Drs. Larry Salkoff and Alice Butler from Washington University Medical

School). The D434G mutation was introduced into the *KCNMA1-pcDNA3* construct by PCR-based site-directed mutagenesis, and confirmed by sequencing analysis of the full *KCNMA1* insert.

To create the expression constructs for *Xenopus* oocyte expression, we subcloned the full-length wild type and mutant *KCNMA1* cDNA into the pSP64 Poly(A) vector (*KCNMA1-pSP64*) using restriction enzymes Hind III and XbaI. To create the expression constructs for CHO cell expression, we subcloned *KCNMA1* cDNA into a GFP vector pIRES2-EGFP (Clontech) with the restriction enzymes NheI and XhoI.

KCNMA1-pSP64 construct was digested with *EcoR I*, and cRNA was prepared using the *In Vitro* Transcription kit with SP6 polymerase. 5 ng of cRNA was injected into each *Xenopus laevis* oocyte 2-6 days before recording. Macroscopic currents were recorded from inside-out patches formed with borosilicate pipettes of 0.9~1.8 megohm resistance. Data were acquired using an Axopatch 200-B patch clamp amplifier (Axon Instruments) and Pulse acquisition software (HEKA Electronik). Records were digitized at 20-μs intervals and low pass filtered at 10 KHz with the Axopatch's 4 pole Bessel filter. Typically, during G-V measurements the series resistance at maximum current amplitude will cause a voltage error of ≤ 5 mV. The error will be smaller at voltages where the activation of channels is not saturated. The shape of the G-V relation and its voltage range affected by this error are smaller than the standard deviation. The pipette solution contained (mM): 140

K-Methanesulfonic Acid, 20 Hepes, 2 KCl, 2 $MgCl_2$, pH 7.20. The basal internal solution contained (mM): 140 K-Methanesulfonic Acid, 20 Hepes, 2 KCl, 1 EGTA, pH 7.20. $CaCl_2$ was added to internal solutions to give the appropriate free $[Ca^{2+}]_i$. All recordings were obtained at room temperature (22-24^oC).

For single channel recordings from Chinese hamster ovary (CHO) cells, *KCNMA1* cDNA (wild type and mutant) were subcloned into a pIRES2-EGFP vector (Clontech) with the restriction enzymes *NheI* and *XhoI*. CHO cells were plated onto coverslips in 12 well Falcon plates, and transfected (0.8 µg DNA/well) using lipofectamine (4 µl/well; Life Technologies) 6-12 hours before recording. Coverslips were placed in a recording chamber on an inverted light microscope (Axiovert 100, Zeiss) and superfused with Ringer solution at 2 ml/min. Transfected cells were selected by visualizing GFP fluorescence. Patch-clamp recordings were made with borosilicate glass electrodes fabricated using a P-97 microelectrode puller (Sutter Instr.). Microelectrodes (20-100 MΩ) were filled with a solution containing (in mM): 144 KCl, 16 NaCl, 2 $MgCl_2$, 2 TES, 11 glucose, 0.065 $CaCl_2$, and 0.08 EGTA. After obtaining a patch, the electrode tip was moved into a separate minichamber, and the inside face of the patch was exposed to the same solution (flow rate 1 ml/min) in which the amount of $CaCl_2$ was varied to give a free calcium concentration of 1, 2, 5, 10, 20, 50, or 100µM (calculated using Webmaxc; www.standford.edu/~cpatton/maxc.html). Recordings of single channel

currents were made in the inside-out configuration from patches with 1-6 channels. These recordings were performed at room temperature in voltage clamp from a holding potential of –60 mV to test potentials from –100 to +100mV (steps of 20 mV for 3 seconds each). Currents were low pass filtered at 2 kHz, and digitized at a rate of 10 kHz using an Axopatch 1D amplifier, Digidata 1322a A/D converter and PClamp software (Axon Instruments). The number of channels in each patch was determined using all points histograms from recordings performed at each level of calcium and voltage. If these histograms did not clearly reveal the number of channels present, the data from that patch were rejected. The open channel probability was analyzed using Clampfit software (Axon Instruments) and the data were fit to the Boltzmann and Hill equations using Origin Software (OriginLab Corp).

3.4 Results

Wild-type and D434G mutant channels were expressed in *Xenopus laevis* oocytes and current-voltage relations were recorded. At a calcium concentration of 2 μM, there was more current induced at the same membrane potential in oocytes expressing D434G mutant channels than in oocytes expressing the wild-type channels (Figure 8a). The voltage dependence of steady-state activation (G-V relation) was shifted to more negative potentials by the D434G mutation, with little change in the slope of the curve. At a calcium concentration of 0.1μM, the G-V relation was shifted

~26 mV toward more negative potential in oocytes expressing the mutant channels. At a calcium concentration of 2 μM, the G-V relation was shifted ~57 mV toward more negative potential by the D434G mutation (Figure 8b). These results indicate that the mutant BK channel has an increased voltage and calcium-dependent activation. Corresponding to the shifts in voltage dependence of activation, the mutant channels were activated faster than the wild-type channels in response to a depolarizing voltage. At a calcium concentration of 2 μM and a test potential of 100 mV, the mutant channels were activated in about 4 ms following the depolarizing voltage pulse, while the wild-type channels were activated in about 7 ms.

These results suggest that during an action potential in neurons, in response to depolarization and calcium entry through voltage-dependent calcium channels, more mutant BK channels open, causing a rapid repolarization of the action potential (72). To better define the mechanism of the increase in macroscopic currents, we made single-channel recordings from BK channels expressed in CHO cells. Both the wild-type channel and the D434G mutant channel were activated by an increase in membrane voltage or in intracellular calcium concentration, but at a given voltage and calcium concentration, the mutant channel was more likely to be in the open state (Figure 9a). At a calcium concentration of 10 μM, the mutant channel was activated at a membrane voltage that is about 50 mV lower than the voltage needed for activation of the wild-type channel. Similar results were

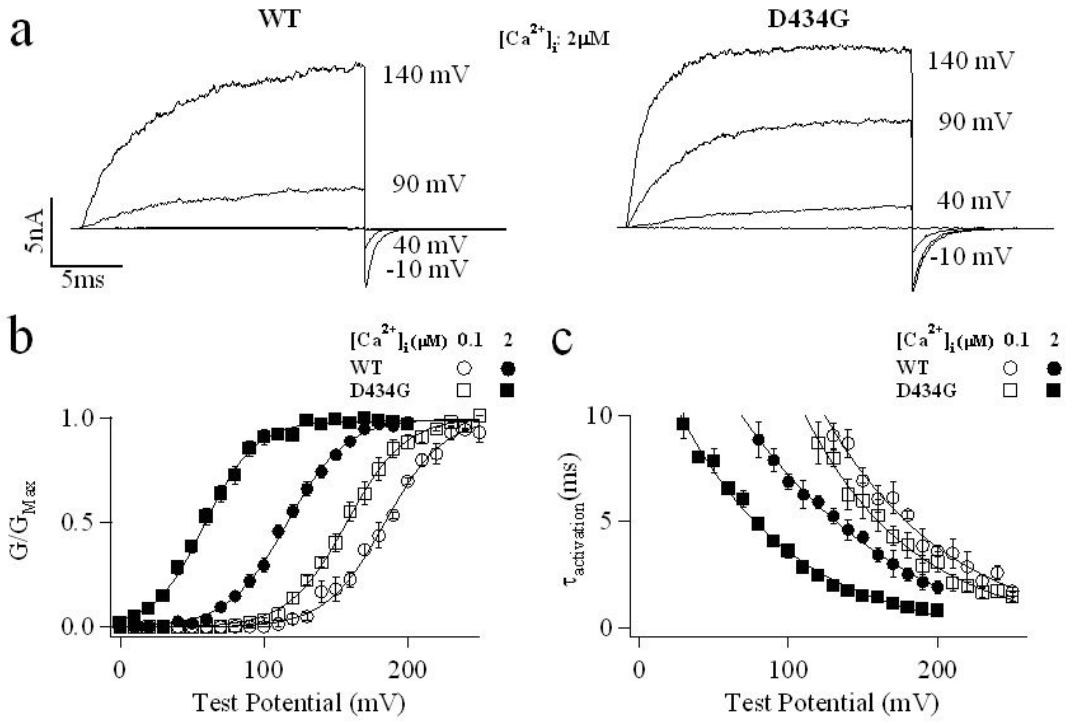

Figure 8. Electrophysiological characterization of wild-type and D434G mutant channels in Xenopus laevis oocytes. a) Selected current traces of WT (left) and D434G mutant (right) channels at 2 μM $[Ca^{2+}]_i$. Test potential were -10 to +140 mV with 50-mV increments. The holding and repolarizing potentials were -80 and -50 mV. b) Mean G-V relations of WT and D434G mutant channels at 0.1 and 2 μM $[Ca^{2+}]_i$. All G-V relations are fitted with the Boltzmann relation (solid lines) with $V_{1/2}$ and slope factor at 2 μM $[Ca^{2+}]_i$: 116 ± 5 mV, 20.6 ± 4.4 for WT and 58.9 ± 4.8 mV, 17.6 ± 4.3 for D434G; and at 0.1 μM $[Ca^{2+}]_i$: 184 ± 8 mV, 20.5 ± 6.3 for WT and 157 ± 5 mV, 20.3 ± 4.2 for D434G. c) Plots of activation time constants of WT and D434G mutant channels as a function of test potential at 0.1 and 2 μM $[Ca^{2+}]_i$. The curves are fitted with an exponential function (solid lines).

obtained at calcium concentration of 2 μM and 50 μM (Figure 9b). These results are consistent with the results from oocytes recordings (Figure 8b).

At membrane voltage of 60 mV and 80 mV, the mutant channel was activated at lower calcium concentrations (Figure 9d). These results suggest the D434G mutation increased calcium sensitivity of the BK channel, which is consistent with the role of the RCK domain as a high affinity site for calcium binding. The relationship between membrane voltage, intracellular calcium concentration and channel activation is shown in Figure 9c. At a given calcium concentration, the mutant channel was activated at lower membrane potentials. At a given membrane potential, the mutant channel was activated at lower calcium concentrations.

Taken together, results from electrophysiological studies in *Xenopus laevis* oocytes and mammalian CHO cells indicate that the D434G mutation leads to enhanced BK channel activation by increasing calcium sensitivity of the RCK domain.

3.5 Discussion

Site-directed mutations of the BK channel were made to search for amino acid residues that are important for calcium binding (73). Beside several residues located in the calcium bowl, M513 near the RCK domain was required to maintain the high-affinity response of the BK channel. M513I resulted in a reduced calcium sensitivity (73), which is opposite to our findings

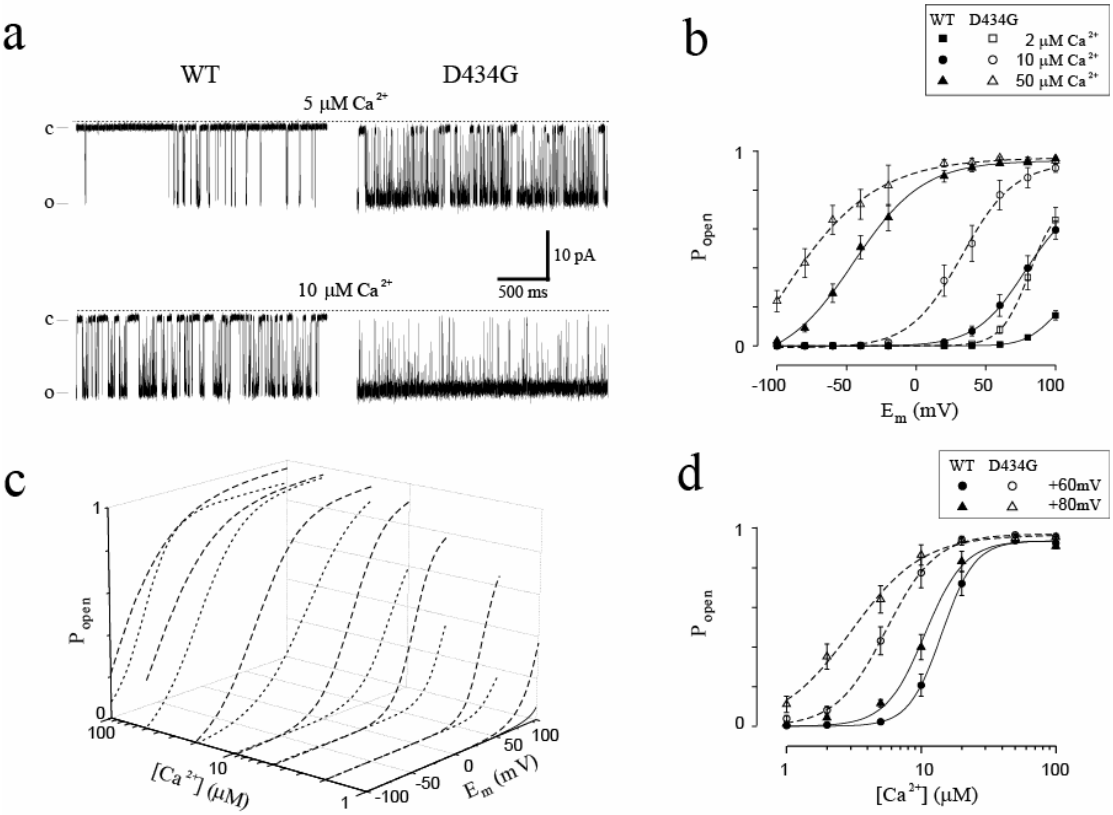

Figure 9. Electrophysiological characterization of wild-type and D434G mutant channels in CHO cells. a) Single-channel currents recorded from WT (left) and D434G mutant channels (right) expressed in CHO cells. At 5 μM (upper traces) and 10 μM (lower traces) calcium concentration, the mutated channel was more likely to be in the open state. There was no difference in single channel conductance. C, closed state; O, open state; dotted lines - zero current level. Membrane potential = +80 mV. b) Effect of membrane potential on P_{open} of WT and mutant D434G channels at three calcium concentrations (2, 10 and 50 μM). Lines are fits to the Boltzmann equation. c) Relationship between calcium concentration, membrane potential, and P_{open}. Each line is the Boltzmann fit obtained as in b. The difference between curves becomes less at high calcium concentration, consistent with saturation of

calcium binding. d) Relationship between P_{open} and calcium concentration at membrane potentials of +60 mV (circles) and +80 mV (triangles) in WT and mutant D434G channels. Lines are fits to the Hill equation. (b-d) solid lines, wild-type; dashed lines, D434G mutant channels. *n* = 5-17 patches for each point.

that the D434G mutation increased calcium sensitivity of the BK channel. One likely explanation is that different mutations result in different conformational change of the BK channel. The conformational change induced by the D434G mutation might favor calcium binding, while the M513I mutation might change the channel conformation in a way that disfavors calcium binding. Structural study may reveal the conformation of the RCK domain of the D434G mutant channel.

It has been reported that calcium sensitivity of the BK channel α subunit can be increased by association with the β subunit. Coexpression of the α and the β subunits of mouse KCNMA1 in *Xenopus laevis* oocytes resulted in increased sensitivity to calcium (74). Similar results were obtained in HEK cells coexpressing the α and the β subunits. It was proposed that the β subunit may increase some of the calcium binding rates in the open channel states (75). A point mutation of human *KCNMB1* encoding the β_1 subunit of the BK channel was identified in patients with hypertension. The mutation resulted in an increased calcium sensitivity of the BK channel, without changes in channel kinetics (76). Taken together, these results indicate that the β subunits of the BK channel play a role in calcium binding. It is likely that binding of the β subunits to the pore-forming α subunits changes the conformation of the calcium-binding domain, thereby increasing calcium sensitivity. It is unknown if coexpression of the D434G mutant channel with different β subunits will further increase calcium sensitivity of the channel,

compared with expression of the D434G mutant channel alone. A synergistic effect on calcium sensitivity between the D434G mutation and the β subunits might exist.

An increase in calcium sensitivity of the BK channel leads to greater macroscopic potassium conductance under physiological conditions. Thus, the D434G mutation results in a gain of function of the α subunit. There are several reasons why gain of function of the BK channel could lead to an increase in brain excitability, causing generalized epilepsy when the thalamus or thalamocortical circuits are involved and paroxysmal dyskinesia when the basal ganglia is involved. The most likely mechanism might be that the D434G mutation leads to faster repolarization of the action potential. Enhanced repolarization enables faster removal of inactivation of sodium channels and thus allows neurons to fire at a higher frequency (77, 78).

Ethanol can activate the BK channel in *C*. elegans (79). This finding may explain the observation that alcohol is one of the factors inducing paroxysmal nonkinesigenic dyskinesia. The D434G mutation may have a synergistic effect with ethanol to trigger the onset of GEPD.

In conclusion, results from the current study demonstrate that the D434G mutation leads to a gain of function of the BK channel by increasing its calcium sensitivity. It is still to be determined how the D434G mutation causes increased calcium sensitivity of the BK channel.

CHAPTER IV

DISCUSSION AND FUTURE DIRECTIONS

The coexistence of epilepsy and paroxysmal dyskinesia in the same individual or family is an increasingly recognized phenomenon. Previous results indicated that the pericentromeric region on chromosome 16 is linked to coexistent epilepsy and paroxysmal dyskinesia (44-48), but no specific gene underlying the phenotype has been identified. By genotyping and linkage analysis, we mapped a genetic locus associated with coexistent generalized epilepsy and paroxysmal dyskinesia on chromosome 10q22. Markers *D10S580* and *D10S1730* in this region showed significant linkage to GEPD with lod scores of 3.68 and 3.73, respectively. The GEPD phenotype described here differs from those linked to chromosome 16 in both the type of seizures and paroxysmal dyskinesia expressed, and linkage to chromosome 16 was not observed. The BK channel is important for neural transmission and muscle contraction. Mice lacking the pore-forming α subunit of BK channel develope

abnormal conditioned eye-blink reflex, impaired locomotion and motor coordination, and high-frequency hearing loss (65, 66). Despite the important physiological roles of BK channel, no mutation in the BK channel gene has been associated with human diseases. We identified a D434G point mutation in the RCK domain of the BK channel α subunit, which cosegregates with all affected individuals in family QW1378, but is absent in all unaffected family members and 500 unrelated healthy controls. Furthermore, D434 of KCNMA1 is evolutionally conserved among different species.

The RCK domain of the α subunit of BK channel has been reported to contain binding sites for calcium and magnesium. We expressed wild-type and D434G mutant BK channels in both *Xenopus laevis* oocytes and CHO cells, and the results from electrophysiological studies indicate that the primary effect of the mutation was to increase calcium sensitivity three- to fivefold, which is consistent with the role of the RCK domain as a high-affinity site for calcium binding. Increased calcium sensitivity might lead to neuronal hyperexcitability *in vivo* by inducing rapid repolarization of action potentials, resulting in GEPD by allowing neurons to fire at a faster rate.

Taken together, these results mapped a new genetic locus associated with coexistent epilepsy and paroxysmal dyskinesia on chromosome 10q22 and established that mutations of the BK channel cause GEPD. This is the first gene that has been associated with coexistent epilepsy and paroxysmal dyskinesia. Our results have implications for the pathogenesis of human

epilepsy, the neurophysiology of paroxysmal dyskinesia and the role of BK channels in neurological disease.

Although epilepsy and paroxysmal dyskinesia are sometimes difficult to differentiate clinically, the current understanding is that they are two distinct disorders with some shared clinical features. The coexistence of epilepsy and paroxysmal dyskinesia in the same individual or family has been reported (42, 43), but the basic pathophysiology underlying this neurological syndrome is unknown, and no specific gene has been associated with it before this study. Coexistence raises the possibility that a common, genetically determined abnormality is variable expressed in the cerebral cortex and in basal ganglia (80).

In the current work, we took advantage of genetic approaches to identify mutated genes in patients affected by epilepsy and/or paroxysmal dyskinesia. We carried out a genome-wide linkage scan with 382 fluorescent microsatellite markers and found two of them, *D10S580* and *D10S1730* on chromosome 10q22, are strongly linked to GEPD syndrome in the family we studied. The lod scores (3.68 for *D10S580* and 3.73 for *D10S1730*) are higher than 3.0, which is considered as evidence for linkage (>99.9%). No other markers showed a lod score of greater than 2.0, indicating that the chromosome 10q22 region was the only region linked to GEPD in the family. By fine mapping and haplotype analysis using eight additional markers, the disease-associated interval was narrowed to a region of 8.4 cM on

chromosome 10q22 flanked by markers *D10S1694 and D10S201*.

Subsequently, we searched the Celera database for genes located in the 8.4 cM region and selected candidate genes for mutational screening by direct sequencing of all the exons. A D434G point mutation was identified in the pore-forming α subunit of the BK channel. This mutation is present in all the affected individuals in family QW1378, but is absent in normal family members and 500 unrelated healthy controls, suggesting that it might contribute to the pathogenesis of GEPD.

Syndromes of coexistent epilepsy and paroxysmal dyskinesia have been reported, including autosomal dominant benigh infantile convulsions and paroxysmal choreoathetosis (ICCA) (44) and related syndromes (46). The ICCA phenotype is characterized by paroxysmal kinesigenic dyskinesia (PKD) and generalized convulsions in infancy and has been linked to chromosome 16p, but the specific gene underlying the phenotype has not been identified yet. The linkage to chromosome 16p was excluded by our linkage study in family QW1378. One likely reason is that the GEPD phenotype described here differs from ICCA in both the type of seizures and paroxysmal dyskinesia expressed. The patients in family QW1378 were diagnosed as paroxysmal nonkinesigenic dyskinesia (PNKD) which is induced by alcohol, caffeine, fatigue and other factors, but not by sudden movement for PKD.

As discussed in Chapter I, mutations in over seventy genes have been linked to different types of epilepsy, and many of these identified genes

encode ion channels (Table I). Our finding of the BK channel mutation in GEPD patients is consistent with the notion that ion channel defects play an important role in the pathogenesis of epilepsy. Our results suggest that ion channel dysfunction might also contribute to the pathogenesis of paroxysmal dyskinesia.

It is likely that BK channel mutations are also associated with epilepsy and/or paroxysmal dyskinesia in other sporadic patients or families. In order to test this hypothesis, we screened BK channel mutations in another family and 102 sporadic patients. However, we did not detect *KCNMA1* mutations in the patients we sequenced. One of the reasons might be that the phenotypes of the patients differ from the GEPD patients. Most of them have either epilepsy or paroxysmal dyskinesia, a few of them have migraine and psychosis, and none of them has coexistent epilepsy and paroxysmal dyskinesia. It is also likely that the mutations are present in different β subunits of the BK channel which could either enhance or inhibit the function of the α subunit. More patient samples will be needed to determine the contribution of BK channelopathy to the pathogenesis of epilepsy and/or paroxysmal dyskinesia.

Although BK channels play important roles in a variety of physiological processes, no mutation in BK channel has been identified that is associated with human diseases before this study. As described in Chapter II, we identified a D434G point mutation in the RCK domain of the α subunit of the

BK channel. In order to investigate how this mutation may lead to GEPD by altering the function of the BK channels, we carried out electrophysiological studies in both *Xenopus laevis* oocytes and CHO cells.

In oocytes, we found that there was more current induced at the same membrane potential in cells expressing D434G mutant channels than in cells expressing the wild-type channels, and the voltage dependence of steady-state activation curve was shifted toward more negative potentials by the D434G mutation. These results indicate that the mutant BK channel has an increased voltage and calcium-dependent activation. Corresponding to the shifts in voltage dependence of activation, the D434G currents activated faster than the wild-type currents in response to a depolarizing voltage pulse. These results suggest that during an action potential in neurons, in response to depolarization and calcium entry through voltage-dependent calcium channel, more mutant BK channels open, causing a rapid repolarization of the action potential (72).

To define better the mechanism of the increase in macroscopic currents in oocytes, we made single-channel recordings from BK channels expressed in CHO cells. Both the wild-type channel and the D434G mutant channel were activated by an increase in voltage or intracellular calcium concentrations, but at a given voltage and calcium concentration, the mutant channel spent substantially more time in the open state. At a given calcium concentration, the mutant channel was activated at lower voltages. These date suggest that

the primary effect of the mutation was to increase calcium sensitivity, rather than to affect the voltage sensor, which is consistent with the role of the RCK domain as a high-affinity site for calcium binding.

It has been reported that ethanol can directly activate the BK channel *in vivo* in C. *elegans* (79). This finding may explain the observation that alcohol triggers paroxysmal dyskinesia in certain individuals in the family reported here and that alcohol is one of the factors that induces paroxysmal nonkinesigenic dyskinesia. The ability of alcohol to trigger PNKD is well recognized, but the detailed mechanism is still under investigation (81). The gain-of-function mutation D434G may have a synergistic effect with ethanol to trigger the onset of the syndromes.

Knockout mice deficient in the BK channel β4 subunit have been created and characterized (67). The β4 subunit is a neuron-specific inhibitory subunit which precludes the BK channel from contributing to the membrane repolarization, resulting in prolonged action potentials and reduced firing rates of neurons. Mice lacking the BK β4 subunit had a gain of function of BK channels, increased firing rate of knockout cells and distinctive seizures emanating from the temporal cortex. Treatment with paxilline, a specific blocker for BK channels, reduced the firing rate. These results support our conclusion that gain of function of the BK channel causes GEPD.

The *in vivo* physiological roles of KCNMA1 remain intriguing. Mice homozygously deficient in *KCNMA1* had abnormal conditioned eye-blink

reflex and abnormal locomotion and motor coordination (65). These mice also developed high-frequency hearing loss at eight weeks of age (66). The phenotype of patients with the *KCNMA1* mutation A1301G seems to be very different from that reported for the knockout mice. One major reason for this difference may be that the human missense mutation is a gain-of-function mutation, whereas the mice lacked BK channels.

In summary, results from our electrophysiological studies and other reports strongly suggest that gain of function of the BK channel may result in generalized epilepsy and paroxysmal dyskinesia by allowing neurons to fire at a faster rate.

As described in Chapter III, the D434G mutation increases the calcium sensitivity of the α subunit, leading to a gain of function of the BK channel. There are several reasons why gain of function of the BK channel could lead to an increase in brain excitability, causing generalized epilepsy when the thalamus or thalamocortical circuits are involved and paroxysmal dyskinesia when the basal ganglia is involved. The most likely mechanism relates to the more rapid repolarization of action potentials by D434G mutant channels. Enhancing this repolarization enables faster repriming (removal of inactivation) of sodium channels and thus allows neurons to fire at a higher frequency (77, 78).

When cells are at rest, the intracellular potential is more negative with respect to the extracellular potential. The potential difference is the resting

membrane potential, which is about -70mV in many mammalian neurons. If progressively larger depolarizing current pulses are applied to the cell membrane, a threshold membrane potential can be reached at which an action potential is triggered. An action potential is a rapid change in the membrane potential followed by a return to the resting membrane potential. An action potential can be divided into a depolarization phase, a repolarization phase and a hyperpolarization phase (Figure 10).

In mammalian neurons, the action potential is triggered by successive opening of sodium and potassium channels in the plasma membrane. When a threshold membrane potential is reached by a depolarizing pulse, the sodium channels open and the potassium channels remain closed. Because the concentration of sodium ions is higher in extracellular fluid than in cytoplasm, sodium ions flow into the cells through sodium channels in the plasma membrane. The influx of positively charged sodium ions makes the inner membrane more positive, resulting in the depolarization phase of an action potential. The sodium conductance peaks at about the same time the action potential peaks, and then the sodium channels begin to close (Figure 10). The potassium channels open more slowly than sodium channels and peak at about the middle of the repolarization phase. Because the concentration of potassium ions is higher in the cytoplasm than in extracellular fluid, potassium ions flow out of the cells through the potassium channels in the plasma membrane. The flow of potassium ions into

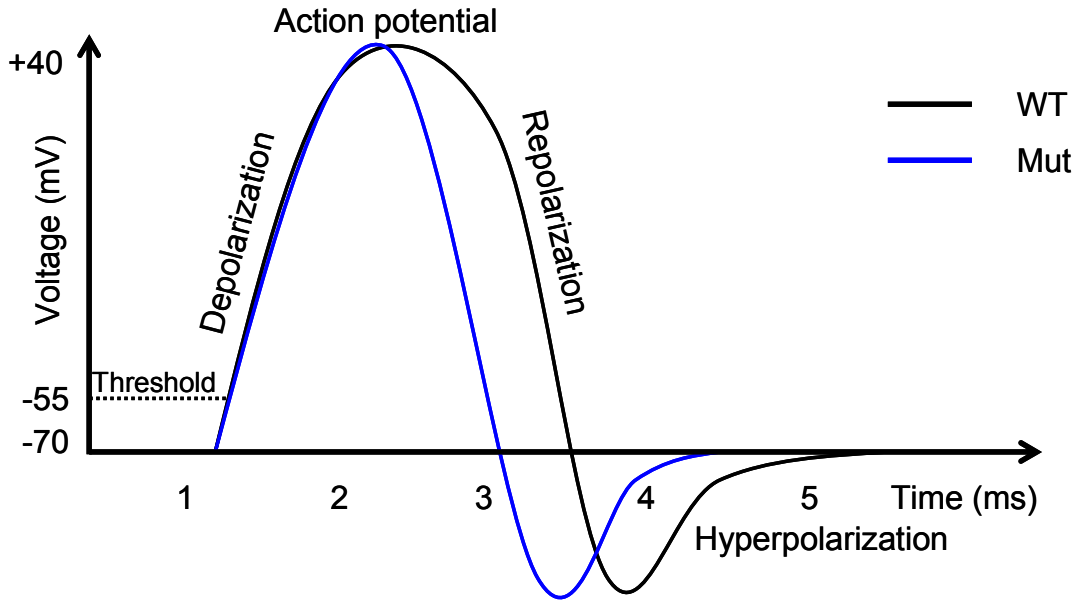

Figure 10. A potential mechanism underlying gain of function of BK channel and GEPD. An action potential is divided into a depolarization phase, a repolarization phase and a hyperpolarization phase. The black curve represents normal action potential. The blue curve represents the action potential involving the D434G mutant BK channels.

fluid results in the repolarization phase of an action potential. When the membrane is returned to the resting membrane potential, all the sodium channels are closed but some of potassium channels are still open. This results in the hyperpolarization phase of an action potential which is more negative than the resting membrane potential. The membrane returns to its resting membrane potential when all potassium channels are closed. One cycle of action potential persists for about 4ms (Figure 10).

An increase in calcium sensitivity of the D434G mutant BK channel leads to greater macroscopic potassium conductance under physiological conditions. At the same membrane potential and intracellular calcium concentration, more mutant channels are likely to open compared with wilt-type channels. Therefore, more potassium ions will flow into the cytoplasm through the mutant BK channels than wild-type channels, resulting in rapid repolarization of action potentials. Enhancing this repolarization enables faster removal of inactivation of sodium channels and thus allows neurons expressing the mutant BK channels to fire at a higher frequency.

There are some other reasons why enhancement of BK channels could lead to GEPD. It is likely that enhancing some inhibitory currents can switch neurons in a circuit into a bursting mode, as can occur with absence seizures that depend on activation of inhibitory $GABA_B$ receptors in the thalamus (82). Likewise, gain of function of BK channels could lead to greater

hyperpolarization and activate the hyperpolarization-activated cation current, resulting in generation of secondary depolarization (83). Another possible explanation is that if BK channels are present in GABAergic neurons, an increase in inhibition of these neurons could lead to disinhibition of a neuronal network.

The studies described in this thesis identified a mutation in the BK channel α subunit that is associated with human GEPD syndrome. These studies lead to a compelling question regarding the role of BK channelopathy in the pathogenesis of epilepsy and/or paroxysmal dyskinesia. Future studies proposed here could address the question and further define how gain of function of BK channels causes GEPD. Specifically, these studies include 1) screening BK channel mutations in other patients with coexistent epilepsy and paroxysmal dyskinesia, 2) investigation of the *in vivo* physiological role of the mutant BK channel in D434G knockin rats, 3) studying the potential synergism between the D434G mutation and the β1 subunit on calcium affinity of the BK channel, 4) determining if the D434G mutation induces a conformational change of the RCK domain.

Different mutations in a single gene could lead to similar pathological phenotypes in patients of different families or populations. For instance, more than twelve mutations of the sodium channel gene *SCN1A* have been identified in patients affected by generalized epilepsy with febrile seizures plus or severe myoclonic epilepsy of infancy. Therefore, it is likely that

KCNMA1 mutations are present in other patients with clinical features that are similar to GEPD in the family we studied.

Future studies will focus on mutational analysis of the twenty-seven exons and adjacent introns of *KCNMA1* using genomic DNA isolated from patients with coexistent epilepsy and paroxysmal dyskinesia. The BK channel β subunits genes (*KCNMB1*, *KCNMB2*, *KCNMB3* and *KCNMB4*) are also good candidates for mutation screening if mutations in *KCNMA1* could not be identified because the β subunits can either enhance or inhibit the function of the α subunit. If different mutations are identified, electrophysiological studies described in Chapter III will be performed to investigate how the mutations may cause the disease. If BK channelopathy is proved to be a common cause of coexistent epilepsy and paroxysmal dyskinesia, BK channel blocking agents might be used as a potential therapy for this syndrome.

The *in vitro* studies described in Chapter III shed light on how the D434G mutation might cause GEPD by enhancing the function of the BK channels, but the functional effect of the mutation *in vivo* is still unknown. If the D434G mutation results in GEPD in human, it might cause phenotypes of epilepsy and/or paroxysmal dyskinesia in animals in which one allele of the normal BK channel gene is replaced by human *KCNMA1* with the mutation.

Rats are commonly used models for studies of epileptic phenotypes because it is easier to record EEG in rats than in mice. Different types of cells (neurons, smooth muscle cells, cardiomyocytes, etc) isolated from

KCNMA1^{D434G}knockin rats and control rats will be used for single channel recordings. The relationship between open channel probability and membrane potential and calcium concentrations will be studied as described in Chapter III. EEG will be recorded from thalamus of KCNMA1^{D434G}Knockin rats as described (86) to determine if there are spike-wave complexes which are observed during epileptic seizures. It will also be examined if there is abnormal movement of limbs in KCNMA1^{D434G}knockin rats treated with alcohol, caffeine, and other factors that have been shown to induce paroxysmal nonkinesigenic dyskinesia in human patients.

The BK channel core formed by four α subunits is necessary for basic conduction function, and association of the core with different β subunits (β1-β4) contributes to the molecular diversity of the BK channel. It has been shown that the β1 subunit interacts with the S0 transmembrane domain and increases the calcium affinity of the BK channel (84, 85), but the molecular mechanism is not clear. Since studies described in Chapter III show that the D434G mutation increases calcium affinity of the BK channel, it is likely that the β1 subunit and the D434G mutation may increase calcium sensitivity in a synergistic way.

Single channel conductance will be recorded in CHO cells expressing the D434G mutant α subunit, wild-type α subunit plus β1 subunit, and D434G mutant α subunit plus β1 subunit. The calcium affinity of each group will be used to determine if a synergism exists between the D434G mutation and the

β1 subunit.

The D434G mutation might induce conformational change of the RCK domain in a way that favors binding of calcium. In order to test this hypothesis, we can purify the mutant RCK domain for structural studies. Because it is technically demanding to purify the whole BK channel, we cloned only the wild-type and mutant RCK domain into His-tagged vector and expressed them in *E.coli*. Although we tried a variety of conditions such as growing *E.coli* at low temperatures, we were unable to obtain native proteins due to the formation of inclusion bodies through interaction of the hydrophobic regions.

An alternative way to obtain soluble native proteins is to express the RCK domain in insect cells where nascent proteins will undergo posttranslational modifications. Posttranslational modifications facilitate proper folding of the proteins which may be soluble with the hydrophobic domains surrounded by the hydrophilic domains. The structure of the mutant RCK domain can be determined by X-ray crystallography.

CHAPTER V

ANGIOGENIC EFFECT OF AGGF1

5.1 Introduction

Blood vessels carry oxygen and nutrients required for normal tissue function throughout our bodies. Angiogenesis, the formation of new blood vessels from the preexisting ones, is a fundamental biological process. In the embryo, blood vessels form through vasculogenesis, a process during which angioblasts differentiate into endothelial cells, which further assemble into a primitive vascular network. In the adult, blood vessel formation occurs under both physiological and pathological conditions (e.g. wound healing, ischemia, etc). Angiogenesis is regulated by an interplay of pro- and anti-angiogenic molecules, and their imbalance could lead to various diseases. For instance, excessive angiogenesis is present in tumors, while insufficient angiogenesis is associated with conditions such as coronary heart disease and stroke.

Unraveling the molecular mechanisms of angiogenesis will help define specific targets for therapeutic intervention.

Vasculogenesis is the process of blood vessel formation in which angioblasts migrate to specific locations and differentiate into endothelial cells which form a primitive vasculature. Vasculogenesis first occurs in the yolk sac blood island of the developing embryo. Within the blood island, hemangioblasts (87), the common precursor for both hematopoietic cells and endothelial cells, differentiate into hematopoietic precursor cells and angioblasts. Several molecules have been implicated in the regulation of hemangioblast differentiation, but the molecular signals are not fully elucidated (88). VEGFR-2 is likely to play an important role at this developmental stage, as mice lacking the receptor failed to develop both hematopoietic and endothelial cell lineages (89).

Angioblasts derived from hemangioblasts migrate to the paraxial mesoderm of yolk sac and differentiate to form a primary capillary plexus. Vasculogenesis was first believed to occur only in the developing embryo. However, it was recently realized that vasculogenesis can also occur postnatally. Circulating bone-marrow derived angioblasts in the adult were identified and able to contribute to neovascularization under conditions such as tumor growth and cardiac ischemia (90-92).

Vasodilation of existing blood vessels is one of the earliest steps in angiogenesis. Vasodilation is accompanied by degradation of extracellular

matrix and an increase in vascular permeability, which allows activated endothelial cells to migrate to distal sites where they assemble to form lumens.

Vascular permeability is mediated by VEGF in response to nitric oxide (93). The vascular permeability activity of VEGF is dependent on Src family kinases (SFKs), as mice deficient in Src or Yes showed no VEGF-induced vascular permeability (94). Increased vascular permeability allows extravasation of plasma proteins that create a provisional scaffold for subsequent migration of activated endothelial cells. Vascular permeability is negatively regulated by Angiopoietin-1 (Ang1) that is a ligand for the endothelial cell-specific receptor Tie2 (95). Ang1 protects the vasculature against excessive plasma leakage, which could result in pathological conditions such as intracranial hypertension and circulatory collapse.

Extracellular matrix must be degraded to free angiogenic factors that are trapped within the matrix and to clear the path for endothelial cells to migrate to distal sites. Many proteinases are involved in this process and matrix metalloproteinases (MMPs) play a central role in degrading extracellular matrix (96). Other proteinases, such as urokinase-type plasminogen activator (u-PA), have also been implicated in matrix degradation (97, 98).

After the extracellular matrix is degraded by proteinases, proliferating endothelial cells are able to migrate to distal sites to assemble into new vessels. VEGF and its homologues play a major role in this step (99, 100).

VEGF induces endothelial cell proliferation through PLC-γ signaling pathway and migration by activating PI3K or FAK. Placental growth factor (PIGF), although dispensable for embryonic vasculogenesis, amplifies VEGF-dependent angiogenesis in the adult (101). VEGF-B and VEGF-C are also involved in endothelial cell proliferation and migration (102, 103).

Beside VEGF and its homologues, several additional molecules have also been implicated in this process. Fibroblast growth factor (FGF)-1 plays an important role in the branching and growth of the coronary arteries, as revealed by studies in FGF-1 transgenic mice (104). Endothelial nitric oxide synthase (eNOS) promotes vessel growth in ischemic hindlimb of mice (105). Transforming growth factor (TGF)-β1 inhibits angiogenesis in tumors (106), and VEGF-induced endothelial cell proliferation is impaired by tumor necrosis factor (TNF), which inhibits the phosphorylation and activation of VEGFR-2 (107). Integrins expressed on the surface of activated endothelial cells regulate endothelial adhesion to the extracellular matrix, which is important for endothelial cell proliferation and migration (108, 109).

Endothelial cells often assemble into solid cords that subsequently acquire a lumen. The length of new blood vessels increases as they fuse with existing vessels. Tumor vessels are structurally distinct from normal vessels in that they are tortuous and dilated with excessive branching. Lumen formation is mainly regulated by VEGF and Ang1 (110), and several integrins are also involved in this process (111).

Endothelial cells become quiescent once new vessels have been assembled and reduced endothelial survival results in vessel regression. VEGF mediates endothelial survival by activating the PI3K/Akt signaling pathway which is further enhanced by VE-cadherin via formation of a multicomponent complex between VE-cadherin, β-catenin, PI3K and VEGFR-2 (112). Ang1 also activates Akt by binding to the Tie-2 receptor and causes increased expression of the apoptosis inhibitor survivin (113). In contrast, Ang2 suppresses endothelial survival in tumors (114). Disruption of interaction between endothelium and extracellular matrix by $\alpha_v\beta_3$ inhibitor results in endothelial apoptosis, but adult quiescent blood vessels are unaffected as $\alpha_v\beta_3$ is only expressed in proliferating cells (115). Endothelial apoptosis can also be induced by some other molecules, including angiostatin, TSP-1, the metallospondin METH-1 and vascular endothelial growth inhibitor.

Maturation of nascent blood vessels involves recruitment of mural cells and development of surrounding matrix which are regulated by a variety of molecules. Mural cells generally refer to as vascular smooth muscle cells and pericytes, both involved in the formation of normal vasculature and responsive to VEGF. PDGFB deficient mice lack pericytes in certain vessels which leads to endothelial hyperplasia, increased capillary diameter and abnormal vascular morphogenesis, indicating that PDGFB signaling through PDGFR-β expressed on mural cells play a role in recruitment of pericytes to

newly formed vessels (116). The phenotypes of EDG1 knockout mice are similar to those of PDGFB deficient mice, suggesting that signaling through EDG1 receptor is another pathway for mural cell recruitment (117). The lack of EDG1 receptor may alter the interaction between endothelial cells and mural cells and interfere with vessel maturation. There might be a crosstalk between the PDGF and EDG receptor signaling involved in mural cell recruitment, as PDGFR-β-deficient mice showed markedly reduced expression of RGS5, a molecule downstream of EDG receptor (118, 119).

Ang1 is known to stabilize nascent vessels and make them less leaky. Recombinant Ang1 restored an organized vasculature and rescued retinal edema and hemorrhage in the absence of mural cells in the retina of mouse neonates (120), suggesting that Ang1 may not be involved in interaction between endothelial cells and mural cells as suggested previously. The role of Ang2 seems to be dependent on VEGF. In the presence of VEGF, Ang2 promotes angiogenesis. In the absence of VEGF, Ang2 acts as an antagonist of Ang1 which destabilizes blood vessels and leads to vessel regression. TGF-β1 plays a role in the establishment and maintenance of vessel wall integrity by promoting extracellular matrix protein deposition and by inducing differentiation of mesenchymal cells into mural cells (121, 122). The TGF-β1-ALK5 signaling pathway induces the plasminogen activator inhibitor 1 which promotes vessel maturation by preventing degradation of extracellular matrix surrounding the nascent vessels. Mice deficient of

Endoglin, a TGF-β-binding protein, showed impaired vascular remolding and differentiation of smooth muscle cells (123).

5.2 Angiogenesis and Angiogenic Factors

VEGF is a key regulator of physiological angiogenesis during embryonic development and pathological angiogenesis associated with tumors, ischemia and other conditions (124). VEGF denotes a family of homodimeric glycoproteins, which consists of five mammalian (VEGF-A, VEGF-B, VEGF-C, VEGF-D, and PIGF) and one virus-encoded member (VEGF-E). They bind to three structurally homologous tyrosine kinase receptors (VEGFR-1, VEGFR-2 and VEGFR-3) in an overlapping pattern (125). Ligand binding induces receptor dimerization and autophosphorylation and, thereby, transduction of signals that regulate cellular function (126). There are also accessory receptors such as neuropilins which enhances the binding of VEGF to VEGFR-2 and VEGF-mediated mitogenic activity for endothelial cells (127).

Disruption of a single VEGF allele in mice resulted in a lethal impairment of vasculogenesis (128, 129), and overexpression of VEGF led to severe abnormalities in heart development and embryonic lethality (130), indicating that VEGF dosage must be tightly regulated to avoid vascular abnormalities. VEGF is also required for angiogenesis in neonatal mice, as evidenced by VEGF inactivation by conditional knockout or by administration of soluble VEGF receptors (131). VEGFR-2 seems to be the major mediator of the

growth and permeability effects of VEGF on vascular endothelial cells. Mice lacking VEGFR-2 failed to develop a functional vasculature and had very few endothelial cells (132). Taken together, these results demonstrate a critical role of VEGF-VEGFR-2 signaling in angiogenesis.

There is increasing evidence that VEGFR-1 may function as a negative regulator of VEGFR-2. Normal vascular development was disrupted by the loss of VEGFR-1 due to obstruction of blood vessels by excessive endothelial cells (133), but deletion of its tyrosine kinase domains did not affect embryonic angiogenesis (134), indicating the role of VEGFR-1 as a decoy receptor that binds to VEGF and thereby controls the amount of VEGF available for VEGFR-2. Such a decoy function might be explained by the soluble form of VEGFR-1 which contains the extracellular ligand-binding domains, but lacks the intracellular tyrosine kinase domains (135). Overexpression of the soluble VEGFR-1 inhibits VEGF-induced migration and proliferation of endothelial cells by forming an inactive complex with VEGF (136).

VEGFR-3 is a high-affinity receptor for VEGF-C and VEGF-D, and activation of VEGFR-3 induces proliferation, migration and survival of lymphatic endothelial cells (137). VEGF-B deficient mice had smaller hearts, suggesting that it might be involved in coronary vascularization and growth (102). VEGF-E is a VEGFR-2-specific ligand encoded by sheep parapoxvirus (138), and transgenic mice overexpressing VEGF-E showed a dramatic

increase in vascularization (139). PIGF deficient mice were healthy and fertile and vascular development in embryos was normal. However, PIGF deficiency impaired VEGF-dependent angiogenesis under pathological conditions such as ischemia and wound healing (140, 141). It is likely that PIGF enhances the activity of VEGF by displacing VEGF from VEGFR-1, thereby increasing the amount of VEGF available to activate VEGFR-2.

Despite the requisite role of VEGF in angiogenesis, some other factors are also involved in this process. The angiopoietin family of proteins, such as Ang1 and Ang2, bind to the Tie receptors that are specifically expressed within the vascular endothelium (142, 143). Mouse embryos lacking Tie-1 failed to establish structural integrity of vascular endothelium resulting in oedema and local haemorrhage, and Tie-2 deficient embryos displayed impaired vascular network formation in endothelial cells (144). Ang1 knockout mice developed a rather normal vasculature during embryogenesis, but this vasculature failed to undergo further remolding processes. In the heart, it was observed that endothelial cells failed to associate appropriately with underlying supporting cells. This finding led to the suggestion that Ang1 plays an important role in mediating reciprocal interactions between the endothelium and surrounding matrix and mesenchyme (145). Vessels in Ang1-overexpressing mice were resistant to leak induced by VEGF or inflammatory agents. This is probably due to the ability of Ang1 to enhance interactions between endothelial cells and their surrounding matrix, as

vessels overexpressing Ang1 were resistant to treatments that normally created holes in the endothelial cell barrier (146). Overexpression of Ang2, another ligand for Tie2, disrupted blood vessel formation in the mouse embryos, indicating that Ang2 is an antagonist for Tie2 (147). Analysis of Ang2 deficient mice indicated that Ang2 is dispensable for embryonic vascular development but is required for postnatal angiogenic remolding (148).

Ephrin-B2 and its EphB4 receptor also play important roles during vascular development (149). Ephrin-B2 is expressed in arterial but not venous endothelial cells, while EphB4 marks veins but not arteries, suggesting that a reciprocal signaling exists between these two types of vessels (150). Mouse embryos lacking ephrin-B2 showed fatal defects in remolding of the embryonic vascular system that are similar to those seen in mice deficient of Ang1 or Tie2 (151). As development proceeds, ephrin-B2 expression extends from the arterial endothelium to surrounding smooth muscle cells and pericytes, suggesting that ephrin-B2 might play a role in the interaction between arterial endothelial cells and mural cells (152, 153).

AGGF1 (angiogenic factor with G patch and FHA domain 1) is a novel angiogenic factor identified by a genetic study of Klippel-Trenaunay syndrome (KTS) (154). AGGF1 contains 714 amino acids with a forkhead-associated (FHA) domain and a G-patch domain. FHA domains are conserved sequences of 65-100 amino acids found primarily within nuclear proteins. It

was shown that the FHA domain mediates protein-protein interactions through its phosphopeptide recognition motif (155). The G-patch domain is found in many eukaryotic proteins and it is often associated with RNA-binding (156).

AGGF1 is expressed in cells involved in angiogenesis, including endothelial cells and vascular smooth muscle cells. Purified AGGF1 promoted blood vessel formation in the chicken embryos similar to VEGF, and the E133K mutation identified in KTS patients further enhanced the angiogenic effect of AGGF1. Consistent with this finding, knockdown of AGGF1 by siRNA inhibited tube formation by endothelial cells plated on matrigel (154). AGGF1 was able to bind to cultured endothelial cells as shown by cell adhesion assays. It is not clear, however, whether AGGF1 acts on endothelial cells in an autocrine fashion or a paracrine fashion as AGGF1 is also expressed by vascular smooth muscle cells. Besides, the receptor for AGGF1 remains to be determined (154). TWEAK is a member of the tumor necrosis factor (TNF) superfamily which has multiple biological activities, including stimulation of cell growth and angiogenesis (157). TWEAK treatment induced proliferation of a variety of human endothelial cells and aortic smooth muscle cells (158). AGGF1 was found to interact with TWEAK by yeast two-hybrid analysis and co-immunoprecipitation assays, and the direct physical interaction between AGGF1 and TWEAK was demonstrated by GST pull-down assays, suggesting that AGGF1 may promote

angiogenesis by interacting with TWEAK (154). Taken together, these results strongly suggest that AGGF1 is a pro-angiogenic factor.

A recent report showed that AGGF1 is a chromatin-associated protein required for β–catenin-mediated transcription and AGGF1 expression was increased in colon tumors, suggesting a role of AGGF1 in tumor angiogenesis (159). The *in vivo* angiogenic effects of AGGF1 remains to be investigated in genetically engineered animal models such as AGGF1 transgenic and knockout mice. Future work on AGGF1 may have important therapeutic implications in treatment of angiogenesis related disorders such as wound healing, ischemic heart disease and cancer.

5.3 Klippel-Trenaunay Syndrome

As discussed in the previous section, AGGF1 is an angiogenic factor involved in the pathogenesis of Klippel-Trenaunay syndrome. A chromosome translocation was identified in a patient affected by KTS and increased AGGF1 expression by 3-fold. We will discuss the clinical features and genetics of KTS in this section.

Klippel-Trenaunay Syndrome (KTS) is a congenital vascular disorder characterized by capillary and venous malformations, extensive distribution of varicose veins and hypertrophy of affected tissues (160, 161). Capillary malformations are the predominant phenotypes of KTS and occur in 98% of the KTS patients. The walls of the capillaries are thin and the endothelial cells

are flat (162). Capillary malformations are sometimes accompanied by venous and lymphatic malformations. Varicose veins account for 72% of the KTS patients (163), which is characterized by dilation, duplication and external compression of veins (164). Limb hypertrophy is present is 67% of KTS patients, and usually involves the lower extremities (163). Hypertrophy can also occur in other parts of the body such as abdomen, head and neck.

Both sporadic and familial cases of KTS have been reported (165, 166). A study of a patient with KTS phenotype and developmental delay and minor anomalies identified a reciprocal translocation t(5;11)(q13.3;p15.1), suggesting a gene responsible for this syndrome might be located to chromosome 5q or 11p (167). Another balanced translocation t(8;14)(q22.3;q13) was identified a patient with a vascular and tissue overgrowth syndrome consistent with KTS (168). A de novo supernumerary ring chromosome derived from chromosome 18 was identified in a patient with KTS and mild mental retardation (169). The identification of three different cytogenetic abnormalities in KTS patients suggest that several different genes may be involved in different cases of KTS. As discussed before, the 5q13.3 breakpoint was found to be located in the promoter region of *AGGF1* and increased the expression of AGGF1 (154). The breakpoints for translocation t(8;14)(q22.3;q13) have been mapped to a 5cM interval on chromosome 8q22.3 and a 1cM interval on chromosome 14q13, but no specific gene has been identified yet (168).

The finding that KTS translocation increases AGGF1 expression suggests that enhanced angiogenesis contributes the pathogenesis of KTS. This is consistent with the increased number and diameter of the venules and defects in the process of vascular growth and remodeling revealed by magnetic resonance imaging (MRI) (170, 171).

CHAPTER VI

AGGF1 TRANSGENIC MICE

6.1 Abstract

AGGF1 has been shown to promote angiogenesis *in vitro*, but its *in vivo* angiogenic effects remain to be investigated. Here we report the generation of AGGF1 transgenic mice using a 2-kb promoter/regulator of the human *AGGF1* gene that showed transcriptional activity by a luciferase assay. The integration of the transgene into the mouse genome was examined by PCR and Southern blot analysis and four positive lines were identified. Unfortunately, no transgene expression was detected by both methods. One likely explanation for this problem is that although the 2-kb promoter/regulator showed transcriptional activity in a sensitive luciferase assay, it might be missing some important enhancer segments that are required for robust transcription *in vivo*. Therefore, it might be better to use a longer promoter fragment up to 8kb, as 98% of known binding sites for mammalian transcription factors occur within 8kb of target genes (172). Alternatively, the Tie-2 promoter could be used to

drive endothelial cell-specific expression of human AGGF1. The Tie-2 promoter has been reported to successfully drive expression of various human genes in transgenic mice, but it might cause loss of phenotypes because AGGF1 is expressed not only in endothelial cells but also vascular smooth muscle cells which are also involved in angiogenesis.

6.2 Introduction

Blood vessels deliver oxygen, nutrients, molecules and cells to all tissues in our body. Small blood vessels consist only of endothelial cells, whereas larger vessels are covered by pericytes and smooth muscle cells. Angiogenesis, the process of growing new blood vessels from the existing vasculature, is essential for organ growth in the embryo and repair of wounded tissue in the adult (173). Angiogenesis is regulated by an interplay of pro- and anti-angiogenic molecules such as VEGFs, angiopoietins and ephrins. If angiogenesis is not properly regulated, it contributes to a number of diseases including cancer, arthritis, stroke and coronary heart disease. Understanding the molecular basis of angiogenesis will have important therapeutic implications. For example, it will be possible to treat ischemic heart disease by stimulating myocardial angiogenesis and cure cancer or inflammatory disorders by inhibiting excessive vessel growth.

AGGF1 is a newly identified protein and there is strong evidence that AGGF1 is a pro-angiogenic factor. AGGF1 is expressed in endothelial cells

and vascular smooth muscle cells, two major components of blood vessels. Purified AGGF1 promoted blood vessel formation in the chicken embryos similar to VEGF, and knockdown of AGGF1 by siRNA inhibited tube formation by endothelial cells plated on matrigel (154). Furthermore, AGGF1 was able to bind to cultured endothelial cells as shown by cell adhesion assay (15). Moreover, AGGF1 was shown to interact with TWEAK directly (154). TWEAK is a member of the tumor necrosis factor (TNF) superfamily which has multiple biological activities, including stimulation of cell growth and angiogenesis (157). Despite these findings, the *in vivo* angiogenic effects of AGGF1 remain to be investigated.

Here we report the generation and genotyping of AGGF1 transgenic mice. The integration of human *AGGF1* into the genome of transgenic mice was confirmed but AGGF1 expression could not be detected by both RT-PCR and Western blot analysis.

6.3 Materials and Methods

The AGGF1 transgene is composed of a 2kb promoter/regulator of human *AGGF1*, a 2.1kb human AGGF1 cDNA and a 600bp human growth hormone (HGH) Poly A. The promoter/regulator region was amplified from genomic DNA by PCR using primers 5'-TGCTGGGCCCTGAGAGAGGAG-3' and 5'-TATACTCGAGGAGCTCCGGCG-3'. The PCR product was purified from agarose gel, digested with enzymes ApaI and XhoI, and cloned into

vector pcDNA3.1(-) digested with ApaI and XhoI. The human AGGF1 cDNA was amplified from pET-28VG5Q (Novagen) using primers 5'-TTCGGCTACAAGTGAGTTTC-3' and 5'-GAAGGACACCTAGTCAGAC-3'. The PCR fragment was purified and cloned into promoter-pcDNA3.1 using enzymes NotI and BamHI. The HGH-Poly A was amplified from Clone 26 (a generous gift from Dr. Jim Gulick, University of Cincinnati Medical Center) using primers 5'-ATATGGATCCGGGTGGCATCCCTGTG-3' and 5'-TATACCTAGGAACAGGCATCTACTGAG-3'. The PCR fragment was cloned into promoter-cDNA-pcDNA3.1 using BamHI. The full-length construct including the promoter/regulator, cDNA, HGH-Poly A and pcDNA3.1(-) vector was verified by direct sequencing and no mutation in the transgene was found. The construct was digested by PmeI to generate the transgene that was used for injection into the pronuclei of fertilized mouse eggs at the Case Transgenic and Targeting Core.

The mouse endothelial cell lines bEnd3 (established from cerebral cortex of adult mouse brain) and C166 (established from yolk sac of mouse embryo) (ATCC, Manassas, VA) were maintained in Dulbecco's modified Eagle's medium (DMEM) containing 10% fetal bovine serum. Cells were cultured at 37 ℃ in a humidified atmosphere with 10% CO_2.

Luciferase reporter assays were performed as described (174). Briefly, bEnd3, C166 and human umbilical vein endothelial cells (HUVEC) were seeded into six-well plates and grown to about 70% confluence. Each well

was cotransfected with 0.9 μg of pGL3-Basic plasmid (Promega) or 0.9 μg of AGGF1(P)-Luc and 0.1 μg of pRL-SV40 plasmid (Promega) using Lipofectamine 2000 (Invitrogen). AGGF1-Luc contains a 2-kb fragment of human AGGF1 promoter/regulator cloned before the luciferase gene of pGL3-Basic. Plasmid pRL-SV40 contains the renilla luciferase gene driven by an SV40 promoter and was cotransfected for normalization. Cells were harvested 24 hours after transfection followed by lysis with passive lysis buffer (Promega). The luciferase activities were measured with the Dual-Luciferase Reporter Assay System (Promega) using a luminometer and normalized by the renilla luciferase activity after subtraction of background. All experiments were performed in triplicates.

Transgenic mice of B6/SJL background were used for genotyping by PCR. Mouse tail tips were isolated from new pups of 4-week old and added to 50 μl of lysis buffer (50 mM Tris-HCl, pH 8.0, 10 mM EDTA, 50 mM NaCl, 0.25% SDS, 0.5 mg/ml Proteinase K). The samples were incubated overnight at 55 ℃ with shaking and diluted in 900 μl H_2O followed by centrifugation at maximal speed for 10 minutes at 4 ℃. The supernatant was collected and used for subsequent PCR. Two pairs of primers were used for PCR: 1) 5'-CTGAAATTACTGATAGCAAC-3' and 5'-GAAGGACACCTAGTCAGAC-3', 2) 5'-TGGTTTTCCGACTGCTTATC-3' and 5'-TTCTCCACCTTCCGCCTTAG-3'. Primer 1 amplifies a 431-bp fragment that includes a portion of human AGGF1 cDNA and HGH poly A. Primer 2

amplifies a 274-bp fragment that includes part of the promoter/regulator segment and the AGGF1 cDNA. The PCR products were resolved on an agarose gel.

The founder mouse lines that are positive by PCR genotyping were verified by Southern blot analysis as described (175). 10 μg of genomic DNA samples from mouse tails were digested with enzymes ApaI and EcoRI and separated on a 0.7% agarose gel overnight at 30 volts. The gel was then denatured in 0.5 N NaOH solutions and DNA was transferred onto a Hybond N+ nylon membrane (Amersham). Membranes were prehybridized with hybridization buffer (50% formamide, 6x SSPE, 5x Denhardt's reagent, 0.5% SDS, 100 μg/ml Salmon Testes DNA) for 1 hour at 42 ℃. The probe that hybridizes to the promoter/regulator fragment of the transgene was amplified by primers (5'-ATGATCTAATTCTAAATGAC-3' and 5'-AACTGTCCTATAGAACTGATG -3') and labeled with ^{32}P using the Random Primer Labeling Kit (Stratagene) according to the manufacturer's instruction. The denatured probe was used for hybridization overnight at 42 ℃ in hybridization oven. The membrane was washed several times before detection by autoradiography.

Total RNA was isolated from different mouse tissues, including the heart, lung, liver, spleen, kidney, brain and embryo, using RNAeasy kit (Qiagen, CA) according to the manufacturer's instructions. The isolated total RNA was digested with DNase at room temperature for 30 minutes to remove potential

genomic DNA contamination. The samples were then reverse transcribed to cDNA by reverse transcriptase. The primers for the reverse transcription step are oliga dT and the oligonucleotide (5'-GAAGGACACCTAGTCAGAC-3') that is complementary to a HGH poly A sequence. The cDNAs were then amplified by PCR using primers and conditions that are the same as described above for genotyping. Mouse β-actin was used as reverse transcription control (the primers were supplied in the RNAeasy kit).

Total proteins were extracted from different mouse tissues stored at a -70°C freezer as described (176). Briefly, mouse tissues were removed from a –70 °C freezer, weighed before thawing, and kept on dry ice. While the samples were still frozen, 800-1000 µl of lysis buffer (1M Tris-HCl pH 8.0, 5M NaCl, 0.1M EDTA, 10% NP-40) were added to each sample (protease inhibitors were added to lysis buffer before use) and the samples were kept on ice for 5 minutes. The samples were then homogenized for 20 seconds and put on ice to keep them cool. This step was repeated 3 to 5 times until the samples were well homogenized. The samples were then kept on ice for 20 minutes followed by centrifugation at 13,000 g at 4 °C for 20 minutes. The supernatant was collected and the protein concentration was measured using absorbance at 280 nm.

For Western blot analysis, the primary antibody we used was a rabbit anti-human AGGF1 antibody (1:500) and the secondary antibody was anti-rabbit IgG-HRP (1:3000). Glyseraldehyde-3-phosphate dehydrogenase

(GAPDH) was used as a loading control.

6.4 Results

The structure of the transgene used for generating transgenic mice overexpressing human AGGF1 is shown in Figure 11a. The transgene cloned in the pcDNA3.1(-) vector is composed of a 2-kb promoter/regulator fragment of human AGGF1 gene, a 2.1-kb human AGGF1 cDNA and a 600-bp human growth hormone (HGH) poly A. the promoter/regulator was used to drive endogenous expression of AGGF1 and HGH poly A was used to stabilize nascent mRNA and facilitate translation (177, 178). The enzymes used for cloning is indicated in Figure 11a.

The promoter activity of the 2-kb promoter/regulator fragment of human AGGF1 gene was examined by a luciferase reporter assay. The relative luciferase activity was measured in human endothelial cell line (HUVEC) and mouse endothelial cell lines (bEnd3 and C166) transfected with AGGF1(P)-Luc containing the 2-kb promoter/regulator fragment. The fragment showed promoter activity in both human and mouse endothelial cells after subtraction of background activity generated by the pGL3-Basic plasmid and normalization (Figure 11b). These results indicate that the promoter/regulator fragment of human AGGF1 gene is likely to drive AGGF1 expression in transgenic mice. The ~4.7-kb transgene was released from the pcDNA3.1 plasmid by digesting with the restriction enzyme PmeI and was

used for injection into mouse fertilized eggs at the Case Transgenic and Targeting Core. Ten lines, eighty-six founder mice of B6/SJL background were generated at the Case Transgenic and Targeting Core. No obvious defects were found in these mice as examined by eyes. Genomic DNA was isolated from the mouse tails and transgene integration was examined by PCR using two pairs of primers. One primer amplifies a 431-bp fragment spanning the promoter and the cDNA and the other primer amplifies a 274-bp fragment including a portion of cDNA and HGH poly A. Clear bands were detected in AGGF1 positive mice, but not in nontransgenic mice, using both primers (Figure 12a).

By PCR genotyping, four positive founder lines (lines 2, 5, 8, 9) were identified, which were further confirmed by Southern blot analysis. Genomic DNA was digested by the enzymes ApaI and EcoRI to release a 2.7-kb fragment including the 2-kb promoter/regulator and part of the cDNA. A ~800-bp probe was designed to hybridize to the promoter/regulator fragment (Figure 11a). A 2.7-kb band representing the transgene was detected in all four positive lines but not in nontransgenic mice (Figure 12b).

The four positive mouse lines were used to examine AGGF1 expression by RT-PCR and Western blot analysis. AGGF1 total RNA and proteins were isolated from various tissues, including the heart, lung, liver, spleen, kidney, brain and embryo. Several pairs of primers were used for RT-PCR, but an

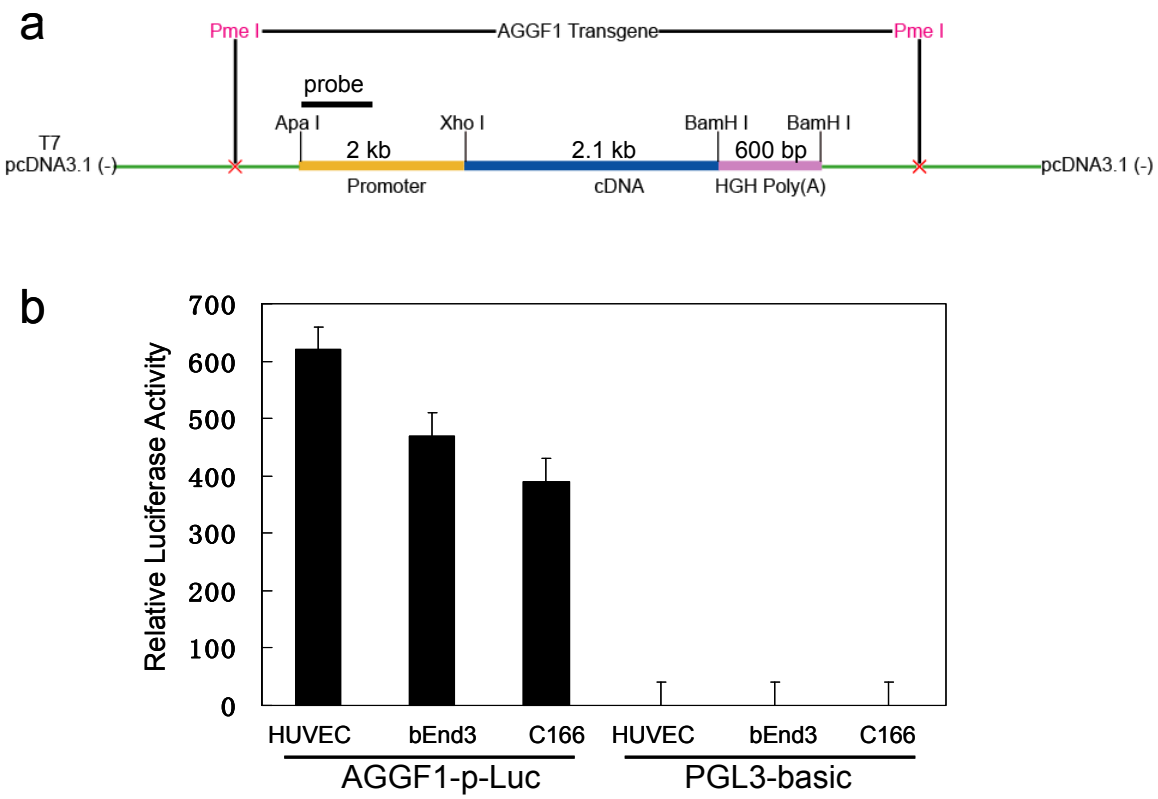

Figure 11. Generation of AGGF1 transgene. a) The AGGF1 transgene contains a 2-kb promoter/regulator fragment of human AGGF1 gene, a 2.1-kb human AGGF1 cDNA and a 600-bp HGH poly A. the transgene is released by PmeI and used for zygote injection. The probe is used for Southern blot. b) The 2-kb promoter/regulator fragment displayed promoter activity by a luciferase reporter assay. The relative luciferase activities of the fragment in human endothelial cell line (HUVEC) and mouse endothelial cell lines (bEnd3 and C166) transfected with AGGF1(P)-Luc were shown. The background activities were measured by transfecting cells with the pGL3-Basic plasmid.

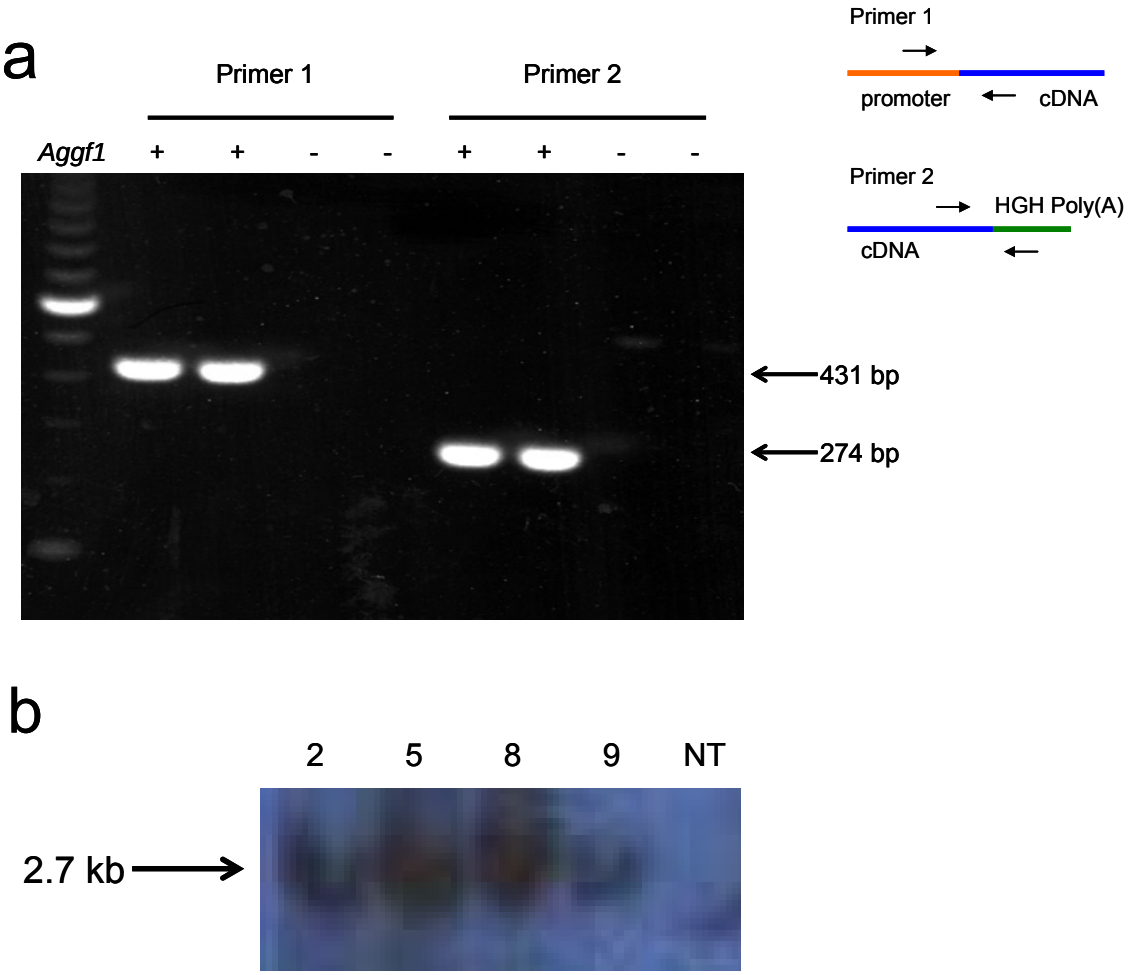

Figure 12. Genotyping of AGGF1 transgenic mice. a) Genotyping by PCR. Primer 1 amplifies a 431-bp fragment that spans the promoter and cDNA in positive mice. Primer 2 amplifies a 274-bp fragment that spans the cDNA and HGH poly A in positive mice. No bands were detected in negative mice. b) Genotyping by southern blot. A 2.7-kb fragment representing the transgene was detected in four positive founder lines (2, 5, 8, 9), but not in nontransgenic mice (NT).

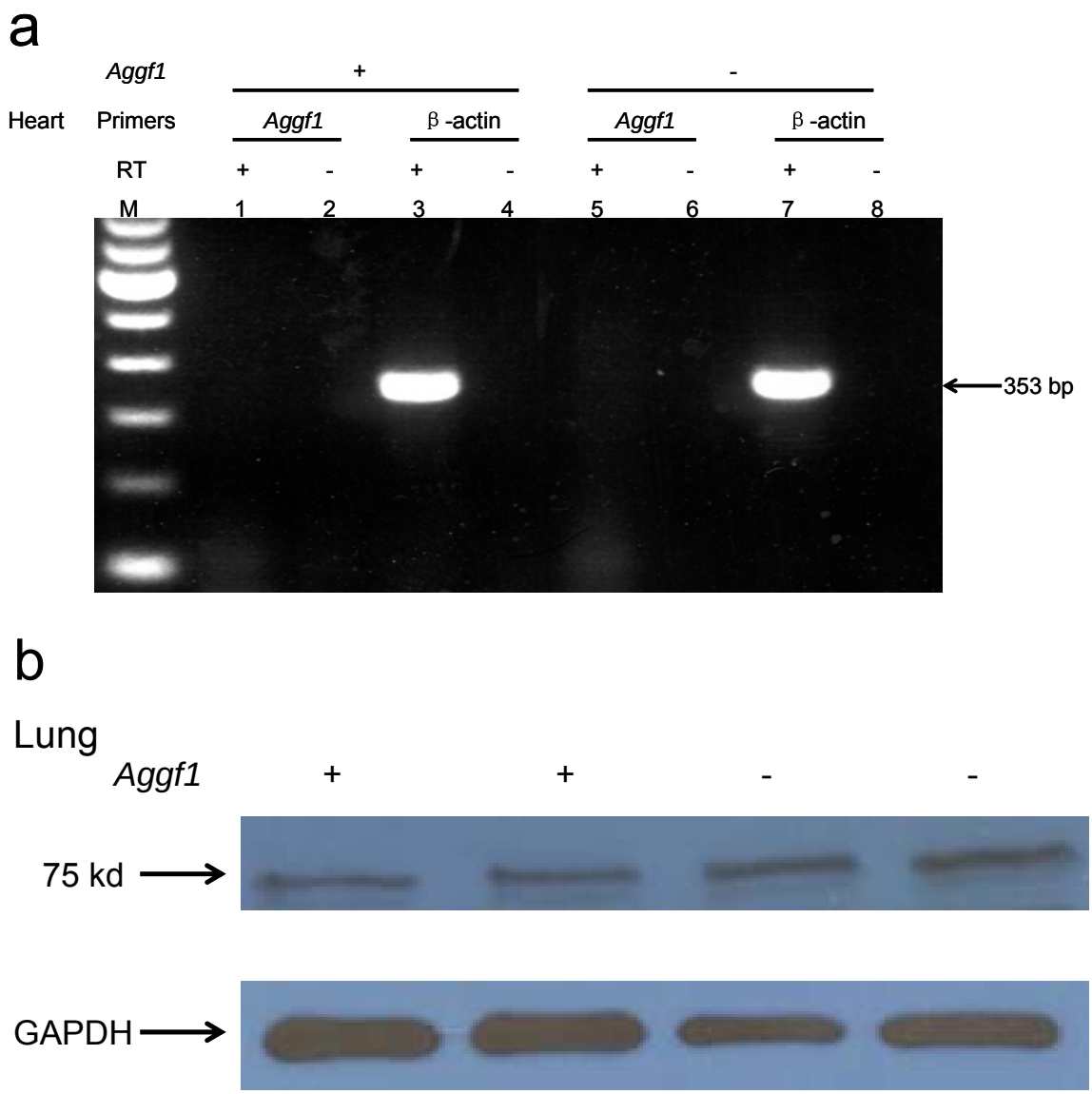

Figure 13. AGGF1 expression in transgenic mice. a) RT-PCR analysis. An expected band was not detected in lane 1. b) Western blot. No increased expression of AGGF1 was detected in AGGF1 transgenic mice.

expected band in lane 1 could not be detected (Figure 13a). RT-PCR results were confirmed by Western blot analysis. The antibody recognizes both human and mouse AGGF1, but an expected increase in band intensity at lane 1 and lane 2 was not detected (Figure 13b). These results indicate that AGGF1 was not expressed in the transgenic mice.

6.5 Discussion

The results from previous *in vitro* studies on AGGF1 indicate that it is a novel angiogenic factor (154). In order to investigate the role of AGGF1 in blood vessel formation *in vivo*, we generated transgenic mice overexpressing human AGGF1 under the control of a 2-kb promoter/regulator fragment of human AGGF1 gene. The purpose of using the promoter/regulator fragment is to mimic endogenous expression of AGGF1.

Integration of transgene into the genome of transgenic mice was confirmed by PCR and Southern blot analysis in four founder lines. The expression of AGGF1 in various tissues was examined by RT-PCR and Western blot analysis, but unfortunately, no AGGF1 expression could be detected.

One possible reason for this problem is that the 2-kb promoter/regulator fragment of human AGGF1 might be missing some important enchancer segments that are required for robust transcription *in vivo*, although the promoter/regulator fragment showed transcriptional activity in a luciferase

reporter assay which is very sensitive. Therefore, a longer promoter fragment up to 8kb could be used to drive transgene expression in transgenic mice, as 98% of known binding sites for mammalian transcriptional factors are located within a 8kb region of target genes. An alternative method would be to use the Tie-2 promoter to drive endothelial cell-specific expression of AGGF1 transgene. Tie-2 promoter has been shown to successfully drive expression of various human genes in transgenic animal models, but it could potentially result in loss of phenotypes in transgenic mice because AGGF1 is expressed not only in endothelial cells but also in smooth muscle cells which are involved in blood vessel formation.

Should transgene expression be achieved, angiogenesis in embryos and various adult tissues will be examined and endothelial cells could be isolated to study cellular process such as proliferation, migration, and survival.

BIBLIOGRAPHY

1. Epilepsy: aetiogy, epidemiology and prognosis. World Health Organization. 2001.
2. Hauser, W. A., Annegers, J. F. & Kurland, L. T. Prevalence of epilepsy in Rochester, Minnesota: 1940-1980. *Epilepsia* **32,** 429-445 (1991).
3. Fisher, R. S. *et al*. Epileptic seizures and epilepsy: definitions proposed by the International League Against Epilepsy (ILAE) and the International Bureau for Epilepsy (IBE). *Epilepsia* **46,** 470-472 (2005).
4. Proposal for revised classification of epilepsies and epileptic syndromes. Commission on Classification and Terminology of the International League Against Epilepsy. *Epilepsia* **30,** 389-399 (1989).
5. Yu, F. H. & Catterall, W. A. Overview of the voltage-gated sodium channel family. *Genome Biol*. **4,** 207 (2003).
6. Isom, L. L., De Jongh, K. S. & Catterall, W. A. Auxiliary subunits of voltage-dependent K^+ channel. *Neuron* **12,** 1183-1194 (1994).
7. Wallace, R. *et al*. Febrile seizures and generalized epilepsy associated with a mutation in the Na^+-channel beta1 subunit gene SCN1B. *Nat. Genet.* **19,** 366-370 (1998).
8. Meadows, L. S. *et al.* Functional and biochemical analysis of a sodium channel beta1 subunit mutation responsible for generalized epilepsy with febrile seizures plus type 1. *J. Neurosci.* **22,** 10699-10709 (2002).
9. Escayg, A. *et al.* Mutations of SCN1A, encoding a neuronal sodium

channel, in two families with GEFS+2. *Nat. Genet.* **24,** 343-345 (2000).

10. Meisler, M. H. & Kearney, J. A. Sodium channel mutations in epilepsy and other neurological disorder. *J. Clin. Invest.* **115,** 2010-2017 (2005).
11. Claes, L. *et al.* De novo mutations in the sodium-channel gene SCN1A cause severe myoclonic epilepsy of infancy. *Am. J. Hum. Genet.* **68,** 1327-1332 (2001).
12. Lossin, C., Wang, D. W., Rhodes, T. H., Vanoye, C. G. & George, A. L. Molecular basis of an inherited epilepsy. *Neuron* **34,** 877-884 (2002).
13. Spampanato, J. *et al.* A novel epilepsy mutation in the sodium channel SCN1A identifies a cytoplasmic domain for beta subunit interaction. *J. Neurosci.* **24,** 10022-10034 (2004).
14. Spampanto, J., Escayg, A., Meisler, M. H. & Goldin, A. L. Functional effects of two voltage-gated sodium channel mutations that cause generalized epilepsy with febrile seizures plus 2. *J. Neurosci.* **21,** 7481-7490 (2001).
15. Heron, S. E. *et al.* Sodium-channel defects in benign familial neonatal-infantile seizures. *Lancet* **360,** 851-852 (2002).
16. Berkovic, S. F. *et al.* Benign familial neonatal-infantile seizures: characterization of a new sodium channelopathy. *Ann. Neurol.* **55,** 550-557 (2004).
17. Mackie, A. R. & Byron, K. L. Cardiovascular KCNQ (Kv7) potassium channels: physiological regulators and new targets for therapeutic

intervention. *Mol Pharmacol* **74,** 1171-1179 (2008).

18. Biervert, C. *et al*. A potassium channel mutation in neonatal human epilepsy. *Science* **279**, 403-406 (1998).
19. Singh, N. A. *et al*. A novel potassium channel gene, *KCNQ2*, is mutated in an inherited epilepsy of newborns. *Nat Genet*. **18**, 25-29 (1998).
20. Charlier, C. *et al*. A pore mutation in a novel KQT-like potassium channel gene in an idiopathic epilepsy family. *Nat genet.* **18**, 53-55 (1998).
21. Zuberi, S. M. *et al*. A novel mutation in the human voltage-gated potassium channel gene (*Kv1.1*) associates with episodic ataxia type 1 and sometimes with partial epilepsy. *Brain* **122**, 817-825 (1999).
22. Smart, S. L. *et al*. Deletion of the K(V)1.1 potassium channel causes epilepsy in mice. *Neuron* **20**, 809-819 (1998).
23. Rho, J. M., Szot, P., Tempel, B. L. & Schwartzkroin, P. A. Developmental seizure susceptibility of kv1.1 potassium channel knockout mice. *Dev Neurosci* **21**, 320-327 (1999).
24. Heilstedt, H. A. *et al.* Loss of the potassium channel beta-subunit gene, KCNAB2, is associated with epilepsy in patients with 1p36 deletion syndrome. *Epilepsia* **42**, 1103-1111 (2001).
25. McCormack, K. *et al*. Genetic analysis of the mammalian K^+ channel beta subunit Kv-beta 2 (Kcnab2). *J. Biol. Chem*. **277**, 219-228 (2002).
26. Jouvenceau, A. *et al*. Human epilepsy associated with dysfunction of the brain P/Q-type calcium channel. *Lancet* **358**, 801-807 (2001).

27. Jun, K. *et al*. Ablation of P/Q-type Ca^{2+} channel currents, altered synaptic transmission, and progressive ataxia in mice lacking the alpha(1A)-subunit. *Proc. Natl. Acad. Sci*. USA **96**, 245-250 (1999).

28. Escayg, A. *et al*. Coding and noncoding variation of the human calcium-channel beta-4 subunit gene CACNB4 in patients with idiopathic generalized epilepsy and episodic ataxia. *Am. J. Hum. Genet*. **66**, 1531-1539 (2000).

29. Barclay, J. *et al*. Ducky mouse phenotype of epilepsy and ataxia is associated with mutations in the Cacna2d2 gene and decreased calcium channel current in cerebellar Purkinje cells. *J Neurosci* **21**, 6095-6104 (2001).

30. Haug, K. *et al*. Mutations in *CLCN2* encoding a voltage-gated chloride channel are associated with idiopathic generalized epilepsies. *Nat Genet* **33**, 527-532 (2003).

31. Bhatia, K. P. Familial (idiopathic) paroxysmal dyskinesias: an update. *Semin Neurol* **21,** 69-74 (2001).

32. Houser, M. K. *et al.* Paroxysmal kinesigenic choreoathetosis: a report of 26 cases. *J Neurol* **246,** 120-126 (1999).

33. Demirkirin, M. & Jankovic, J. Paroxysmal dyskinesias: clinical features and classification. *Ann Neurol* **4,** 571-579 (1995).

34. Bhatia, K. P. *et al.* Paroxysmal exercise induced dystonia: eight new cases and a review of the literature. *Mov Disord* **12,** 1007-1012 (1997).

35. Browne, D. L. *et al.* Episodic ataxia/myokymia syndrome is associated with point mutations in the human potassium channel gene, KCNA1. *Nat Genet* **8,** 136-140 (1994).

36. Ophoff, R. A. *et al.* Familial hemiplegic migraine and episodic ataxia type-2 are caused by mutations in the ca^{2+} gene CACNL1A4. *Cell* **87,** 543-552 (1996).

37. Fouad, G. T. *et al.* A gene for familial paroxysmal dyskinesia (FPD1) maps to chromosome 2q. *Am J Hum Genet* **59,** 135-139 (1996).

38. Fink, J. K. *et al.* Paroxysmal dystonic choreoathetosis: tight linkage to chromosome 2q. *Am J Hum Genet* **59,** 140-145 (1996).

39. Lee, W. L. *et al.* Association of infantile convulsions with paroxysmal dyskinesias (ICCA syndrome): confirmation of linkage to human chromosome 16p12-q12 in a Chinese family. *Hum Genet* **103,** 608-612 (1998).

40. Tomita, H. *et al.* Paroxysmal kinesigenic choreoathetosis locus maps to chromosome 16p11.2-q12.1. *Am J Hum Genet* **65,** 1688-1697 (1999).

41. Fahn, S. The paroxysmal dyskinesias. *Movement Disorders* **3,** 310-345 (1994).

42. Guerrini, R. Idiopathic epilepsy and paroxysmal dyskinesia. Epilepsia 42, 36-41 (2001).

43. Guerrini, R. et al. Early-onset absence epilepsy and paroxysmal dyskinesia. Epilepsia 43, 1224-1229 (2002).

44. Szepetowski, P. *et al.* Familial infantile convulsions and paroxysmal choreoathetosis: a new neurological syndrome linked to pericentromeric region of human chromosome 16. *Am J Hum Genet* **61,** 889-898 (1997).
45. Swoboda, K. J. *et al.* Paroxysmal kinesigenic dyskinesia and infantile convulsions. Clinical and linkage studies. *Neurology* **55,** 224-230 (2000).
46. Guerrini, R. *et al.* Autosomal recessive rolandic epilepsy with paroxysmal exercise-induced dystonia and writer's cramp: delineation of the syndrome and gene mapping to chromosome 16p12-11.2. *Ann Neurol* **45,** 344-352 (1999).
47. Bennett, L. B., Roach, E. S. & Bowcock, A. M. Locus for paroxysmal kinesigenic dyskinesia maps to human chromosome 16. *Neurology* **54,** 125-130 (2000).
48. Valente, E. M. *et al.* A second paroxysmal kinesigenic choreoathetosis locus (EKD2) mapping on 16q13-q22.1 indicates a family of genes which give rise to paroxysmal disorders on human chromosome 16. *Brain* **123,** 2040-2045 (2000).
49. Pallotta, B. S., Magleby, K. L. & Barrett, J. N. Single channel recordings of Ca^{2+}-activated K^+ currents in rat muscle cell culture. *Nature* **293,** 471-474 (1981).
50. Knaus, H. G. *et al.* Distribution of high conductance Ca^{2+}-activated K^+ channels in rat brain: targeting to axons and nerve terminals. *J Neurosci* **16,** 955-963 (1996).

51. Issa, N. P. & Hudspeth, A. J. Clustering of Ca^{2+} channels and Ca^{2+}-activated K^+ channels at fluorescently labeled presynaptic active zones of hair cells. *Proc. Natl. Acad. Sci.* **91,** 7578-7582 (1994).
52. Barrett, J. N., Magleby, K. L. & Pallotta, B. S. Properties of single calcium-activated potassium channels in cultured rat muscle. *J Physiol* **331,** 211-230 (1982).
53. McCobb, D. P. *et al.* A human calcium-activated potassium channel gene expressed in vascular smooth muscle. *Am. J. Physiol.* **269,** 767-777 (1995).
54. Meera, P., Wallner, M., Song, M. & Toro, L. Large conductance voltage- and calcium-dependent K^+ channel, a distinct member of voltage-dependent ion channels with seven N-terminal transmembrane segments (S0-S6), an extracellular N terminus, and an intracellular (S9-S10) C terminus. *Proc. Natl. Acad. Sci.* **94,** 14066-14071 (1997).
55. Schreiber, M. & L, Salkoff. A novel calcium-sensing domain in the BK channel. *Biophys J* **73,** 1355–1363 (1997).
56. Xia, X., Zeng, X. & Lingle, C. J. Multiple regulatory sites in large-conductance calcium-activated potassium channels. *Nature* **418,** 880-884 (2002).
57. Shi, J. *et al.* Mechanism of magnesium activation of calcium-activated potassium channels. *Nature* **418,** 876-879 (2002).
58. Ma, Z., Lou, X. J. & Horrigan, F. T. Role of charged residues in the S1-S4

voltage sensor of BK channels. *J. Gen. Physiol.* **127,** 309-328 (2006).

59. Bezanilla, F. The voltage sensor in voltage-dependent ion channels. *Physiol Rev* **80,** 555-592 (2000).

60. Cui, J., Cox, D. H. & Aldrich, R. W. Intrinsic voltage dependence and Ca^{2+} regulation of mSlo large conductance Ca-activated K^+ channels. *J. Gen. Physiol.* **109,** 647-673 (1997).

61. Ahern, A. & Horn, R. Specificity of charge-carrying residues in the voltage sensor of potassium channels. *J. Gen. Physiol.* **123,** 205-216 (2004).

62. Wei, A., Solaro, C., Lingle, C. & Salkoff, L. Calcium sensitivity of BK-type K_{Ca} channels determined by a separable domain. *Neuron* **13,** 671-681 (1994).

63. Ye, S., Li, Y., Chen, L. & Jiang, Y. Crystal structures of a ligand-free MthK gating ring: insights into the ligand gating mechanism of K^+ channels. *Cell* **126,** 1161-1173 (2006).

64. Horrigan, F. T. & Aldrich, R. W. Coupling between voltage sensor activation, Ca2+ binding and channel opening in large conductance (BK) potassium channels. *J. Gen. Physiol.* **120,** 267-305 (2002).

65. Sausbier, M. *et al.* Cerebellar ataxia and Purkinje cell dysfunction caused by Ca^{2+}-activated K^+ channel deficiency. *Proc. Natl. Acad. Sci.* **101,** 9474-9478 (2004).

66. Ruttiger, L. *et al.* Deletion of the Ca^{2+}-activated potassium (BK) alpha-subunit but not the BK beta1-subunit leads to progressive hearing

loss. *Proc. Natl. Acad. Sci.* **101,** 12922-12927 (2004).

67. Brenner, R. *et al.* BK channel beta4 subunit reduces dentate gyrus excitability and protects against temporal lobe seizures. *Nat Neurosci* **8,** 1752-1759 (2005).

68. Brenner, R. *et al*. Vasoregulation by the beta1 subunit of the calcium-activated potassium channel. *Nature* **407,** 870-876 (2000).

69. Seibold, M. A. *et al.* An African-specific functional polymorphism in KCNMB1 shows sex-specific association with asthma severity. *Hum. Mol. Genet.* **17,** 2681-2690 (2008).

70. Eunson, L. H. *et al.* Clinical, genetic, and expression studies of mutations in the potassium channel gene KCNA1 reveal new phenotypic variability. *Ann Neurol* **48,** 647-656 (2000).

71. Noebels, J. L. The biology of epilepsy genes. *Annu. Rev. Neurosci.* **26,** 599-625 (2003).

72. Adams, P. R., Constanti, A., Brown, D. A. & Clark, R. B. Intracellular Ca^{2+} activates a fast voltage-sensitive K^+ current in vertebrate sympathetic neurons. *Nature* **296,** 746-749 (1982).

73. Bao, L., Rapin, A. M., Holmstrand, E. C. & Cox, D. H. Elimination of the BK(Ca) channel's high-affinity Ca(2+) sensitivity. *J. Gen. Physiol.* **120,** 173-189 (2002).

74. McManus, O. B. *et al.* Functional role of the beta subunit of high conductance calcium-activated potassium channels. *Neuron* **14,** 645-650

(1995).

75. Nimigean, C. M. & Magleby, K. L. The beta subunit increases the Ca^{2+} sensitivity of large conductance Ca^{2+}-activated potassium channels by retaining the gating in the bursting states. *J. Gen. Physiol.* **113,** 425-440 (1999).

76. Fernandez-Fernandez, J. M. *et al.* Gain-of-function mutation in the KCNMB1 potassium channel subunit is associated with low prevalence of diastolic hypertension. *J. Clin. Invest.* **113,** 1032-1039 (2004).

77. Jin, W., Sugaya, A., Tsuda, T., Ohguchi, H. & Sugaya, E. Relationship between large conductance calcium-activated potassium channel and bursting activity. *Brain Res* **860,** 21-28 (2000).

78. Lancaster, B. & Nicoll, R. A. Properties of two calcium-activated hyperpolarizations in rat hippocampal neurons. *J Physiol* **389,** 187-203 (1987).

79. Davies, A. G. *et al.* A central role of the BK potassium channel in behavioral responses to ethanol in *C. elegans*. *Cell* **115,** 655-666 (2003).

80. Guerrini, R., Parmeggiani, L. & Casari, G. Epilepsy and paroxysmal dyskinesia: co-occurrence and differential diagnosis. *Adv Neurol* **89,** 433-441 (2002).

81. Lee, H. Y. *et al.* The gene for paroxysmal non-kinesigenic dyskinesia encodes an enzyme in a stress response pathway. *Hum. Mol. Genet.* **13,** 3161-3170 (2004).

82. von Krosigk, M., Bal, T. & McCormick, D. A. Cellular mechanisms of a synchronized oscillation in the thalamus. *Science* **261,** 361-364 (1993).
83. McCormick, D. A. & Pape, H. C. Properties of a hyperpolarization-activated cation current and its role in rhythmic oscillation in thalamic relay neurons. *J Physiol* **431,** 291-318 (1990).
84. Cox, D. H. & Aldrich, R. W. Role of the β1 subunit in large-conductance Ca^{2+}-activated K^{+} channel gating energetics. *J Gen Physiol* **116,** 411-432 (2000).
85. Wallner, M., Meera, P. & Toro, L. Determinant for beta-subunit regulation in high-conductance voltage-activated and Ca^{2+}-sensitive K^{+} channels: an additional transmembrane region at the N terminus. Proc. Natl. Acad. Sci. **93,** 14922-14927 (1996).
86. Meeren, H. K. *et al.* Thalamic lesions in a genetic rat model of absence epilepsy: dissociation between spike-wave discharges and sleep spindles. *Exp Neurol* **217,** 25-37 (2009).
87. Choi, K. Hemangioblast development and regulation. *Biochem Cell Biol* **76,** 947-956 (1998).
88. Carmeliet, P. Development biology. Controlling the cellular brakes. *Nature* **401,** 657-658 (1999).
89. Shalaby, F. *et al.* Failure of blood-island formation and vasculogenesis in Flk-1-deficient mice. *Nature* **376,** 62-66 (1995).
90. Asahara, T. *et al.* VEGF contributes to postnatal neovascularization by

mobilizing bone marrow-derived endothelial progenitor cells. *EMBO J* **18,** 3964-3972 (1999).

91. Kalka, C. *et al.* Vascular endothelial growth factor (165) gene transfer augments circulating endothelial progenitor cells in human subjects. *Circ Res* **86,** 1198-1202 (2000).
92. Rafii, S. Circulating endothelial precursors: mystery, reality, and promise. *J Clin Invest* **105,** 17-19 (2000).
93. Kimura, H. *et al.* Hypoxia response element of the human vascular endothelial growth factor gene mediates transcriptional regulation by nitric oxide: control of hypoxia-inducible factor-1 activity by nitric oxide. *Blood* **95,** 189-197 (2000).
94. Eliceiri, B. P. *et al.* Selective requirement for Src kinases during VEGF-induced angiogenesis and vascular permeability. *Mol Cell* **4,** 915-924 (1999).
95. Thurston, G. et al. Angiopoietin-1 protects the adult vasculature against plasma leakage. Nat Med 6, 1-4 (2000).
96. Nelson, A. R., Fingleton, B., Rothenberg, M. L. & Matrisian, L. M. Matrix metalloproteinases: biologic activity and clinical implications. *J Clin Oncol* **18,** 1135-1149 (2000).
97. Heymans, S. *et al.* Inhibition of plasminogen activators or matrix metalloproteinases prevents cardiac rupture but impairs therapeutic angiogenesis and causes cardiac failure. *Nat Med* **5,** 1135-1142 (1999).

98. Carmeliet, P. & Collen, D. Development and disease in proteinase-deficient mice: role of the plasminogen, matrix metalloproteinase and coagulation system. *Thromb Res* **91,** 255-285 (1998).

99. Ferrara, N. Vascular endothelial growth factor and the regulation of angiogenesis. *Recent Prog Horm Res* **55,** 15-35 (2000).

100. Veikkola, T., Karkkainen, M., Claesson-Welsh, L. & Alitalo, K. Regulation of angiogenesis via vascular endothelial growth factor receptors. *Cancer Res* **60,** 203-212 (2000).

101. Persico, M. G., Vincenti, V. & DiPalma, T. Structure, expression and receptor-binding properties of placenta growth factor (PIGF). *Curr Top Microbiol Immunol* **237,** 31-40 (1999).

102. Bellomo, D. *et al.* Mice lacking the vascular endothelial growth factor-B (vegfb) have smaller hearts, dysfunctional coronary vasculature, and impaired recovery from cardiac ischemia. *Circ Res* **86,** E29-E35 (2000).

103. Eriksson, U. & Alitalo, K. Structure, expression and receptor-binding properties of novel vascular endothelial growth factors. *Curr Top Microbiol Immunol* **237,** 41-57 (1999).

104. Fernandez, B. *et al.* Transgenic myocardial overexpression of fibroblast growth factor-1 increases coronary artery density and branching. *Circ Res* **87,** 207-213 (2000).

105. Murohara, T. *et al.* Nitric oxide synthase modulates angiogenesis in response to tissue ischemia. *J Clin Invest* **101,** 2567-2578 (1998).

106. Gohongi, T. *et al.* Tumor-host interactions in the gallbladder suppress distal angiogenesis and tumor growth: involvement of transforming growth factor beta1. *Nat Med* **5,** 1203-1208 (1999).

107. Guo, D. Q. *et al.* Tumor necrosis factor employs a protein-tyrosine phosphatase to inhibit activation of KDR and vascular endothelial cell growth factor-induced endothelial cell proliferation. *J Biol Chem* **275,** 11216-11221 (2000).

108. Eliceiri, B. P. & Cheresh, D. A. The role of alphav integrins during angiogenesis. *Mol Med* **4,** 741-750 (1998).

109. Eliceiri, B. P. & Cheresh, D. A. The role of alphav integrins during angiogenesis: insights into potential mechanisms of action and clinical development. *J Clin Invest* **103,** 1227-1230 (1999).

110. Suri, C. *et al.* Increased vascularization in mice overexpressing angiopoietin-1. *Science* **282,** 468-471 (1998).

111. Bayless, K. J. Salazar, R. & Davis, G. E. RGD-dependent vacuolation and lumen formation observed during endothelial cell morphogenesis in three-dimensional fibrin matrices involves the alpha(v)beta(3) and alpha(5)beta(1) integrins. *Am J Pathol* **156,** 1673-1683 (2000).

112. Carmeliet, P. *et al.* Targeted deficiency or cytosolic truncation of the VE-cadherin gene in mice impairs VRGF-mediated endothelial survival

and angiogenesis. *Cell* **98,** 147-157 (1999).

113. Papapetropoulos, A. *et al.* Angiopoietin-1 inhibits endothelial cell apoptosis via the Akt/surviving pathway. *J Biol Chem* **275,** 9102-9105 (2000).

114. Holash, J. *et al*. Vessel cooption, regression, and growth in tumors mediated by angiopoietins and VEGF. *Science* **284,** 1994-1998 (1999).

115. Varner, J. A. Brooks, P. C. & Cheresh, D. A. Review: The integrin $\alpha_v\beta_3$: angiogenesis and apoptosis. *Cell Adhesion Communication* **3,** 367-374 (1995).

116. Hellstrom, M. *et al.* Lack of pericytes leads to endothelial hyperplasia and abnormal vascular morphogenesis. *J Cell Biol* **153,** 543-553 (2001).

117. Kluk, M. J. & Hla, T. Signaling of sphingosine-1-phosphate via the S1P/EDG-family of G-protein-coupled receptors. *Biochim Biophys Acta* **1582,** 72-80 (2002).

118. Kluk, M. J. Colmont, C. Wu, M. T. & Hla, T. Platelet-derived growth factor (PDGF)-induced chemotaxis does not require the G protein-coupled receptor S1P1 in murine embryonic fibroblasts and vascular smooth muscle cells. *FEBS Lett* **533,** 25-28 (2003).

119. Cho, H., Kozasa, T., Bondjers, C., Betsholtz, C. & Kehrl, J. H. Pericyte-specific expression of Rgs5: implications for PDGF and EDG receptor signaling during vascular maturation. *FASEB J* **13,** 440-442 (2003).

120. Uemura, A. *et al.* Recombinant angiopoietin-1 restores higher-order architecture of growing blood vessels in mice in the absence of mural cells. *J Clin Invest* **110,** 1619-1628 (2002).

121. Pepper, M. S. Transforming growth factor-β: vasculogenesis, angiogenesis, and vessel wall integrity. *Cytokine Growth Factor Rev* **8,** 21-43 (1997).

122. Chambers, R. C., Leoni, P., Kaminski, N., Laurent, G. J. & Heller, R. A. Global expression profiling of fibroblast responses to transforming growth factor-beta1 reveals the induction of inhibitor of differentiation-1 and provides evidence of smooth muscle cell phenotypic switching. *Am J Pathol* **162,** 533-546 (2003).

123. Goumans, M. J. *et al.* Balancing the activation state of the endothelium via two distinct TGF-β type 1 receptors. *EMBO J* **21,** 1743-1753 (2002).

124. Ferrara, N. VEGF and the quest for tumor angiogenesis factors. *Nat Rev Cancer* **2,** 795-803 (2002).

125. Yancopoulos, G. D. *et al.* Vascular-specific growth factors and blood vessel formation. *Nature* **407,** 242-248 (2000).

126. Cross, M. J., Dixelius, J., Matsumoto, T. & Claesson-Welsh, L. VEGF-receptor signal transduction. *Trends Biochem Sci* **28,** 488-494 (2003).

127. Soker, S., Takashima, S., Miao, H., Neufeld, G. & Klagsbrun, M.

Neuropilin-1 is expressed by endothelial and tumor cells as an isoform-specific receptor for vascular endothelial growth factor. *Cell* **92,** 735-745 (1998).

128. Carmeliet, P. *et al.* Abnormal blood vessel development and lethality in embryos lacking a single VEGF allele. *Nature* **380,** 435-439 (1996).

129. Ferrara, N. *et al.* Heterozygous embryonic lethality induced by targeted inactivation of the VEGF gene. *Nature* **380,** 439-442 (1996).

130. Miquerol, L., Langille, B. L. & Nagy, A. Embryonic development is disrupted by modest increases in vascular endothelial growth factor gene expression. Development 127, 3941-3946 (2000).

131. Gerber, H. P. *et al.* VEGF is required for growth and survival in neonatal mice. *Development* **126,** 1149-1159 (1999).

132. Shalaby, F. *et al.* Failure of blood-island formation and vasculogenesis in FlK-1-deficient mice. *Nature* **376,** 62-66 (1995).

133. Fong, G., Rossant, J., Gertsenstein, M. & Breltman, M. L. Role of the Flt-1 receptor tyrosine kinase in regulating the assembly of vascular endothelium. *Nature* **376**, 66-70 (1995).

134. Hiratsuka, S., Minowa, O., Kuno, J., Noda, T. & Shibuya, M. Flt-1 lacking the tyrosine kinase domain is sufficient for normal development and angiogenesis in mice. *Proc. Natl. Acad. Sci. USA* **95**, 9349-9354 (1998).

135. Kendall, R. L., Wang, G. & Thomas, K. A. Identification of a natural

soluble form of the vascular endothelial growth factor receptor, FLT-1, and its heterodimerization with KDR. *Biochem. Biophys. Res. Commun*. **226**, 324-328 (1996).

136. Kendall, R. L. & Thomas, K. A. Inhibition of vascular endothelial growth factor activity by an endogenously encoded soluble receptor. *Proc. Natl. Acad. Sci. USA* **90**, 10705-10709 (1993).

137. Makinen, T. *et al*. Isolated lymphatic endothelial cells transducer growth, survival and migratory signals via the VEGF-C/D receptor VEGFR-3. *EMBO J*. **20**, 4762-4773 (2001).

138. Ogawa, S. *et al*. A novel type of vascular endothelial growth factor: VEGF-E (NZ-7 VEGF) preferentially utilizes KDR/Flk-1 receptor and carries a potent mitotic activity without heparin-binding domain. *J. Biol. Chem*. **273**, 31273-31282 (1998).

139. Kiba, A., Sagara, H., Hara, T. & Shibuya, M. VEGFR-2-specific ligand VEGF-E induces non-edematous hyper-vascularization in mice. *Biochem. Biophys. Res. Commun*. **301**, 371-377 (2003).

140. Park, J. E., Chen, H. H., Winer, J., Houck, K. A. & Ferrara, N. Placenta growth factor. Potentiation of vascular endothelial growth factor bioactivity, *in vitro* and *in vivo*, and high affinity binding to Flt-1 but not to Flk-1/KDR. *J. Biol. Chem*. **269**, 25646-25654 (1994).

141. Carmeliet, P. *et al*. Synergism between vascular endothelial growth factor and placental growth factor contributes to angiogenesis and plasma

extravasation in pathological conditions. *Nature Med*. **7**, 575-583 (2001).

142. Sato, T. N., Qin, Y., Kozak, C. A. & Audus, K. L. tie-1 and tie-2 define another class of putative receptor tyrosine kinase genes expressed in early embryonic vascular system. *Proc Natl Acad Sci USA* **90,** 9355-9358 (1993).

143. Korhonen, J. et al. Enhanced expression of the tie receptor tyrosine kinase in endothelial cells during neovascularization. Blood 80, 2548-2555 (1992).

144. Sato, T. N. *et al.* Distinct roles of the receptor tyrosine kinases Tie-1 and Tie-2 in blood vessel formation. *Nature* **376,** 70-74 (1995).

145. Suri, C. *et al.* Requisite role of Angiopoietin-1, a ligand for the Tie2 receptor, during embryonic angiogenesis. *Cell* **87,** 1171-1180 (1996).

146. Thurston, G. *et al*. Leakage-resistant blood vessels in mice transgenically overexpressing angiopoietin-1. *Science* **286,** 2511-2514 (1999).

147. Maisonpierre, P. C. *et al.* Angiopoietin-2, a natural antagonist for Tie2 that disrupts in vivo angiogenesis. *Science* **277,** 55-60 (1997).

148. Gale, N. W. *et al.* Angiopoietin-2 is required for postnatal angiogenesis and lymphatic patterning, and only the latter role is rescued by Angiopoietin-1. *Dev Cell* **3,** 302-304 (2002).

149. Gale, N. W. & Yancopoulos, G. D. Growth factors acting via endothelial cell-specific receptor tyrosine kinases: VEGFs, angiopoietins,

and ephrins in vascular development. *Genes Dev* **13,** 1055-1066 (1999).

150. Wang, H. U., Chen, Z. & Anderson, D. J. Molecular distinction and angiogenic interaction between embryonic arteries and veins revealed by ephrin-B2 and its receptor Eph-B4. *Cell* **93,** 741-753 (1998).

151. Adams, R. H. *et al.* Roles for ephrinB ligands and EphB receptors in cardiovascular development: demarcation of arterial/venous domains, vascular morphogenesis, and sprouting angiogenesis. *Genes Dev* **13,** 295-306 (1999).

152. Gale, N. W. *et al.* Ephrin-B2 selectively marks arterial vessels and neovascularization sites in the adult, with expression in both endothelial and smooth-muscle cells. *Dev Biol* **230,** 151-160 (2001).

153. Shin, D. *et al.* Expression of ephrinB2 identifies a stable genetic difference between arterial and venous vascular smooth muscle as well as endothelial cells, and marks subsets of microvessels at sites of adult neovascularization. *Dev Biol* **230,** 139-150 (2001).

154. Tian, X. *et al.* Identification of an angiogenic factor that when mutated causes susceptibility to Klippel-Trenaunay syndrome. *Nature* **427,** 640-645 (2004).

155. Durocher, D., Henckel, J., Fersht, A. R. & Jackson, S. P. The FHA domain is a modular phosphopeptide recognition motif. *Mol Cell* **4,** 387-394 (1999).

156. Guglielmi, B. & Werner, M. The yeast homolog of human PinX1 is

involved in rRNA and small nucleolar RNA maturation, not in telomere elongation inhibition. *J Biol Chem* **277,** 35712-35719 (2002).

157. Wiley, S. R. & Winkles, J. A. TWEAK, a member of the TNF superfamily, is a multifunctional cytokine that binds the TweakR/Fn14 receptor. *Cytokine Growth Factor Rev* **14,** 241-249 (2003).

158. Lynch, C. N. *et al.* TWEAK induces angiogenesis and proliferation of endothelial cells. *J Biol Chem* **274,** 8455-8459 (1999).

159. Major, M. B. *et al.* New regulators of Wnt/β-catenin signaling revealed by integrative molecular screening. *Sci Signal* **1,** ra12 (2008).

160. Klippel, M. & Trenaunay, P. Du naevus variqueux osteo-hypertrophique. *Arch Gen Med* **185,** 641-672 (1900).

161. Berry, S. A. *et al.* Klippel-Trenaunay syndrome. *Am J Med Genet* **79,** 319-326 (1998).

162. Vikkula, M., Boon, L, M., Mulliken, J. B. & Olsen, B. R. Molecular basis of vascular anomalies. *Trends Cardiovasc Med* **8,** 281-292 (1998).

163. Jacob, A. G. Klippel-Trenaunay syndrome: spectrum and management. *Mayo Clin Proc* **73,** 28-36 (1998).

164. Gloviczki, P. *et al*. Klippel-Trenaunay syndrome: the risks and benefits of vascular interventions. *Surgery* **110,** 469-479 (1991).

165. Ceballos-Quintal, J. M., Pinto-Escalante, D. & Castillo-Zapata, I. A new case of Klippel-Trenaunay-Weber (KTW) syndrome: evidence of autosomal dominant inheritance. *Am J Med Genet* **63,** 426-427 (1996).

166. Lorda-Sanchez, I., Prieto, L., Rodriguez-Pinilla, E. & Martinez-Frias, M. L. Increased parental age and number of pregnancies in Klippel-Trenaunay-Weber syndrome. *Ann Hum Genet* **62,** 235-239 (1998).

167. Whelan, A. J., Watson, M. S., Porter, F. D. & Steiner, R. D. Klippel-Trenaunay-Weber syndrome associated with a 1:11 balanced translocation. *Am J Med Genet* **59,** 492-494 (1995).

168. Wang, Q. *et al.* Identification and molecular characterization of de novo translocation t(8;14)(q22.3;q13) associated with a vascular and tissue overgrowth syndrome. *Cytogenet Cell Genet* **95,** 183-188 (2001).

169. Timur, A. A. *et al.* Identification and molecular characterization of a de novo supernumerary ring chromosome 18 in a patient with Klippel-Trenaunary syndrome. *Ann Hum Genet* **68,** 353-361 (2004).

170. Baskerville, P. A., Ackroyd, J. S. & Browse, N. L. The etiology of the Klippel-Trenaunay syndrome. *Ann Surg* **202,** 624-627 (1985).

171. Fontana, A. & Olivetti, L. Peripheral MR angiography of Klippel-Trenaunay syndrome. *Cardiovasc Intervent Radiol* **27,** 297-299 (2004).

172. Boyer, L. A. *et al.* Core transcriptional regulatory circuitry in human embryonic stem cells. *Cell* **122,** 947-956 (2005).

173. Carmeliet, P. Angiogenesis in life, disease and medicine. *Nature* **438,** 932-936 (2005).

174. Li, H. & Forstermann, U. Structure-activity relationship of

staurosporine analogs in regulating expression of endothelial nitric-oxide synthase gene. *Mol Pharmacol* **57,** 427–435 (2000).

175. Huen, D. S., Fox, A., Kumar, P. & Searle, P. F. Dilated heart failure in transgenic mice expressing the Epstein-Barr virus nuclear antigen-leader protein. *J Gen Virol* **74,** 1381-1391 (1993).

176. Dignam, J. D. Preparation of extracts from higher eukaryotes. *Methods in Enzymology*. **182**, 194-203 (1990).

177. Huez, G. *et al.* Role of the polyadenylate segment in the transition of globin messenger RNA in Xenopus oocytes. *Proc Natl Acad Sci USA* **71,** 3143-3146 (1974).

178. Munroe, D. & Jacobson, A. mRNA poly(A) tail, a 3' enhancer of translational initiation. *Mol Cell Biol* **10,** 3441-3455 (1990).

179. Rosahl, T. W. *et al.* Essential functions of synapsins I and II in synaptic vesicle regulation. *Nature* **375,** 488-493 (1995).

180. Crowder, K. M. *et al*. Abnormal neurotransmission in mice lacking synaptic vesicle protein 2A (SV2A). *Proc Natl Acad Sci USA* **96,** 15268-15273 (1999).

181. Kash, S. F. *et al.* Epilepsy in mice deficient in the 65-kDa isoform of glutamic acid decarboxylase. *Proc Natl Acad Sci USA* **94,** 14060-14065 (1997).

182. Sepkuty, J. P. *et al*. A neuronal glutamate transporter contributes to neurotransmitter GABA synthesis and epilepsy. *J Neurosci* **22,** 6372-6379

(2002).

183. Waymire, K. G. *et al.* Mice lacking tissue non-specific alkaline phosphatase die from seizures due to defective metabolism of vitamin B-6. *Nat Genet* **11,** 45-51 (1995).

184. Cossette, P. *et al.* Mutation of GABAR1 in an autosomal dominant form of juvenile myoclonic epilepsy. *Nat Genet* **31,** 184-189 (2002).

185. Baulac, S. *et al.* First genetic evidence of GABA(A) receptor dysfunction in epilepsy: a mutation in the gamma2-subuint gene. *Nat Genet* **28,** 46-48 (2001).

186. Wallace, R. H. *et al.* Mutant GABA(A) receptor gamma2-subunit in childhood absence epilepsy and febrile seizures. *Nat Genet* **28,** 49-52 (2001).

187. Harkin, L. A. *et al.* Truncation of the GABA(A) receptor gamma2 subunit in a family with generalized epilepsy with febrile seizures plus. *Am. J. Hum. Genet.* **70,** 530-536 (2002).

188. Kananura, C. *et al.* A splice-site mutation in GABRG2 associated with childhood absence epilepsy and febrile convulsions. *Arch Neurol* **59,** 1137-1141 (2002).

189. Brusa, R. *et al.* Early-onset epilepsy and postnatal lethality associated with an editing-deficient GluR-B allele in mice. *Science* **270,** 1677-1680 (1995).

190. Bertrand, D. *et al.* How mutations in the nAChRs can cause ADNFLE

epilepsy. *Epilepsia* **43,** 112-122 (2002).

191. Brennan, T. J. *et al*. Sound-induced seizures in serotonin 5-HT2c receptor mutant mice. *Nat Genet* **16,** 387-390 (1997).

192. Tecott, L. H. *et al.* Eating disorder and epilepsy in mice lacking 5-HT2c serotonin receptors. *Nature* **374,** 542-546 (1995).

193. Lee, H. Y. *et al.* The gene for paroxysmal non-kinesigenic dyskinesia encodes an enzyme in a stress response pathway. *Hum Mol Genet* **13,** 3161-3170 (2004).

194. Suls, A. *et al.* Paroxysmal exercise-induced dyskinesia and epilepsy is due to mutations in SLC2A1, encoding the glucose transporter GLUT1. *Brain* **131,** 1831-1844 (2008).

195. Weber, Y. G. *et al.* GLUT1 mutations are a cause of paroxysmal exercise-induced dyskinesias and induce hemolytic anemia by a cation leak. *J Clin Invest* **118,** 2157-2168 (2008).